

Lipid remodeling in phytoplankton exposed to multi-environmental drivers in a mesocosm experiment

Sebastian I. Cantarero¹, Edgart Flores¹, Harry Allbrook¹, Paulina Aguayo^{2,3,4}, Cristian A. Vargas^{3,5}, John E. Tamanaha⁶, J. Bentley C. Scholz⁶, Lennart T. Bach⁷, Carolin R. Löscher^{8,9}, Ulf Riebesell¹⁰, Balaji Rajagopalan¹¹, Nadia Dildar¹, Julio Sepúlveda^{1,5}

¹Department of Geological Sciences and Institute of Arctic and Alpine Research (INSTAAR), University of Colorado Boulder, Boulder, CO 80309, USA

²Departamento de Oceanografía, Universidad de Concepción, Casilla 160-C, Concepción, Chile

³Department of Aquatic System, Faculty of Environmental Sciences & Environmental Sciences Center EULA Chile, Universidad de Concepción, Concepción 4070386, Chile

⁴Institute of Natural Resources, Faculty of Veterinary Medicine and Agronomy, Universidad de Las Américas, Sede Concepcion, Chacabuco 539, Concepcion 3349001, Chile

⁵Millennium Institute of Oceanography (IMO), Universidad de Concepción, Concepción 4070386, Chile

⁶Laboratory for Interdisciplinary Statistical Analysis, Department of Applied Mathematics, University of Colorado, Boulder, Boulder CO, 80309, USA

⁷Institute for Marine and Antarctic Studies, University of Tasmania, Hobart, TAS 7004, Australia

⁸Nordcee, Department of Biology, University of Southern Denmark, Odense, Denmark

⁹Danish Institute for Advanced Study, University of Southern Denmark, Odense, Denmark

¹⁰Marine Biogeochemistry, GEOMAR Helmholtz Centre for Ocean Research Kiel, Düsternbrooker Weg 20, D-24105, Kiel, Germany

¹¹Department of Civil, Environmental, and Architectural Engineering, University of Colorado-Boulder, Boulder, CO, USA

Correspondence to: Sebastian I. Cantarero (sebastian.cantarero@colorado.edu)

Abstract. Lipid remodeling, the modification of cell membrane chemistry via structural rearrangements within the lipid pool of an organism, is a common physiological response amongst all domains of life to alleviate environmental stress and maintain cellular homeostasis. Whereas culture experiments and environmental studies of phytoplankton have demonstrated the plasticity of lipids in response to specific abiotic stressors, few analyses have explored the impacts of multi-environmental stressors at the community-level scale. Here, we study changes in the pool of intact polar lipids (IPLs) of a phytoplanktonic community exposed to multi-environmental stressors during a ~2-month long mesocosm experiment deployed in the eastern tropical South Pacific off the coast of Callao, Perú. We investigate lipid remodeling of IPLs in response to changing nutrient stoichiometries, temperature, pH, and light availability in surface and subsurface water-masses with contrasting redox potentials, using multiple linear regressions, classification and regression trees, and random forest analyses. We observe proportional increases of certain glycolipids (namely mono- and di-galactosyldiacylglycerols; MG and DG, respectively) associated with higher temperatures and oxic conditions, consistent with previous observations of their utility to compensate for thermal stress, and their degradation under oxygen stress. N-bearing (i.e., betaine lipids and phosphatidylethanolamine; BL and PE) and non-N-bearing (i.e., MG, phosphatidylglycerol, and sulfoquinovosyldiacylglycerol; PG, SQ) IPLs are anti-correlated, and have strong positive correlations with nitrogen repleted and depleted conditions, respectively, which suggests a substitution mechanism for N-bearing IPLs under nitrogen limitation. Reduced CO₂(aq) availability and increased pHs are associated with greater proportions of DG and sulfoquinovosyldiacylglycerol (SQ) IPLs, possibly in response to the lower concentration of CO₂(aq) and the overall lower availability of inorganic carbon for fixation. A higher production of MG in surface waters corresponds well with their established photoprotective and antioxidant mechanisms in thylakoid membranes. The observed statistical relationships between IPL distributions, physicochemical parameters, and the composition of the phytoplankton community suggest evidence of lipid remodeling in response to environmental stressors. These physiological

45 responses may allow phytoplankton to reallocate resources from structural or extrachloroplastic membrane lipids (i.e.,
46 phospholipids and betaine lipids) under high-growth conditions, to thylakoid/plastid membrane lipids (i.e., glycolipids and
47 certain phosphatidylglycerols) under growth-limiting conditions. Further investigation of the exact mechanisms controlling
48 the observed trends in lipid distributions are necessary to better understand how membrane reorganization under multi-
49 environmental stressors can affect the pools of cellular C, N, P, and S, as well as their fluxes to higher trophic levels in marine
50 environments subjected to increasing environmental pressure. Our results suggest that future studies addressing the
51 biogeochemical consequences of climate change in the Eastern Tropical South Pacific Ocean must take into consideration the
52 impacts of lipid remodeling in phytoplankton.

53 **1 Introduction**

54 The Eastern Tropical South Pacific (ETSP) is one of the most productive eastern boundary upwelling systems in the world
55 (Chavez and Messié, 2009) and harbors one of the largest oxygen deficient zones (ODZs) (Fuenzalida et al., 2009; Ulloa and
56 Pantoja, 2009; Thamdrup et al., 2012). Global warming has led to the expansion of ODZs over the recent decades and they are
57 expected to continue expanding due to the reduction in oxygen solubility with increasing temperature (Stramma et al., 2008;
58 Stramma et al., 2010; Gilly et al., 2013), as well as because of enhanced ocean stratification and reduced ventilation of the
59 ocean's interior (Keeling et al., 2010). The future behavior of the ETSP upwelling system in a warmer world remains uncertain;
60 increases in wind-induced upwelling intensity and duration (Gutiérrez et al., 2011; Bakun et al., 2010) may increase the supply
61 of nutrients to the surface in coastal regions, whereas enhanced thermal stratification may reduce nutrient supply in the open
62 ocean (Behrenfeld et al., 2006). Furthermore, upwelling regions are prone to highly variable pH (Capone and Hutchins, 2013),
63 and the global ocean will experience a decreasing average pH as more CO₂ accumulates in the atmosphere and is absorbed by
64 the ocean (Jiang et al., 2019). Accordingly, major shifts in marine planktonic community composition, turnover rates (Henson
65 et al., 2021), and adaptations (Irwin et al., 2015) are expected in future scenarios of ocean conditions, which are expected to
66 lead to cascading effects on ocean biogeochemistry and marine ecosystems (Hutchins and Fu, 2017).

67
68 Primary productivity in the ETSP is predominantly regulated by the wind-induced upwelling of nutrients, light availability,
69 and Fe limitation (Messié and Chavez, 2015). Thus, changes in the supply of inorganic N along the upwelling region of the
70 ETSP are likely to induce significant shifts in the phytoplankton community composition. Longer upwelling seasons along
71 nearshore environments could further stimulate productivity of fast-growing eukaryotic algae that currently dominate these
72 systems (e.g., diatoms; Messié et al., 2009). However, shorter upwelling seasons or weaker upwelling currents could favor
73 more survivalist or mixotrophic algae, in addition to N-fixing diazotrophs that thrive under widespread nitrogen limitation
74 (Dutkiewicz et al., 2012). The rate of primary productivity in the surface ocean not only affects the supply of sinking organic
75 matter and thus oxygen consumption via microbial respiration in the subsurface (Wyrski, 1962), but also results in a shift of
76 redox potentials that drive substantial losses of bioavailable N under reducing conditions at intermediate depths (Lam et al.,
77 2009; Wright et al., 2012). Additionally, expected changes in ocean warming and stratification (Huertas et al., 2011; Morán et
78 al., 2010; Yvon-Durocher, 2015), lowered dissolved oxygen concentration (Wu et al., 2012), and decreased pH (Dutkiewicz
79 et al., 2015, Bach et al., 2017), will disrupt phytoplanktonic assemblages differently based on their individual tolerances and

80 physiological plasticity. However, little is known of the physiological adaptations of phytoplankton on a community-level
81 scale in response to multi environmental stressors.

82

83 Phytoplankton have been shown to activate several lipid-based physiological mechanisms in response to environmental stimuli
84 (Li-Beisson et al., 2019; Sayanova et al., 2017; Kong et al., 2018). In fact, intact Polar Lipids (IPLs) are a class of membrane
85 lipids characterized by a polar head group typically attached to a glycerol backbone from which aliphatic chains are attached
86 via ester and/or ether bonds (Sturt et al., 2004; Lipp et al., 2008; Schubotz et al., 2009; Van Mooy and Fredricks, 2010).
87 Dominant planktonic lipid classes include phospholipids with a phosphate-bearing polar head group (e.g., phosphatidylcholine
88 PC; phosphatidylethanolamine PE; and Phosphatidylglycerol PG), glycolipids featuring a sugar moiety in the polar head (e.g.,
89 monoglycosyldiacylglycerol MG; diglycosyldiacylglycerol DG; sulfoquinovosyldiacylglycerol SQ), and betaine lipids with a
90 quaternary amine positively charged and attached to lipid chains (e.g. diacylglyceryl hydroxymethyl-trimethyl- β -alanine
91 DGTA; diacylglyceryl trimethylhomoserine DGTS; and diacylglycerylcarboxy-N-hydroxymethyl-choline DGCC) (Kato et
92 al., 1996; Rütters et al., 2001; Zink et al., 2003; Suzumura, 2005; Van Mooy et al., 2006). The remodeling of IPLs, the main
93 constituents of cell and organellar membranes, provides numerous physiological adjustments to attenuate environmental
94 stressors impacting phytoplankton (Zienkiewicz et al., 2016). These include nutrient limitation (Van Mooy et al., 2009; Meador
95 et al., 2017; Abida et al., 2015; Wang et al., 2016), homeoviscous regulation in response to changing temperature (Sato et al.,
96 1980; Sinensky, 1974; Neidleman, 1987) and pH (Tatsuzawa and Takizawa 1996; Poerschmann et al., 2004; Guckert and
97 Cooksey, 1990; Jin et al., 2021), or photosynthetic function under varying light availability (Sato et al., 2003; Gašparović et
98 al., 2013; Khotimchenko and Yakovleva, 2005). While IPL distributions in environmental studies are typically used as
99 chemotaxonomic biomarkers that trace the presence and abundance of specific microbial groups (Sturt et al., 2004; Schubotz
100 et al., 2009; Van Mooy and Fredricks, 2010), their distributions have been used in conjunction with additional microbial or
101 geochemical measurements to assess how microbial metabolisms contribute to the chemical environment (Van Mooy et al.,
102 2009; Wakeham et al., 2012; Schubotz et al., 2018; Cantarero et al., 2020). Yet, few studies have explored how multiple
103 environmental drivers impact IPL remodeling at the community level and in time series, and the associated adaptability of
104 phytoplankton to environmental change.

105

106 Lab-based culture experiments have been a major step forward in understanding how lipid remodeling may impact a
107 biogeochemical system (as summarized above). However, a significant challenge remains in contextualizing these findings at
108 the community scale. Conversely, observational studies from direct measurements of natural systems are often logistically
109 limited in temporal scale, and consequently, do not fully capture the dynamics and heterogeneity of biogeochemical conditions.
110 Mesocosms are experimental apparatuses at the interface between controlled culture experiments and environmental
111 observations that allow for the examination of natural systems and entire ecosystems under semi-controlled conditions to
112 explore the impacts of a changing climate and ocean system (Riebesell et al., 2013). Here, we study changes in the composition,
113 diversity, and abundance of phytoplanktonic IPLs in response to changes in the biological, physical, and chemical composition

114 of a marine ecosystem subjected to semi-controlled conditions in a 2-month long mesocosm experiment off the coast of Perú.
115 We investigate the potential for IPL remodeling amongst phytoplankton in response to multiple environmental stressors
116 including nutrient availability, O₂ concentration, pH, temperature, and light availability to highlight adaptation strategies
117 available to phytoplankton in response to a changing ocean system.
118

119 **2 Methods**

120 **2.1 Mesocosm Deployment and Sampling**

121 On February 22, 2017, eight “Kiel Off-Shore Mesocosms for Ocean Simulations” (KOSMOS; Riebesell et al., 2013) were
122 deployed just north of Isla San Lorenzo, 6 km off the Peruvian coastline (12.0555° S, 77.2348° W; Fig. 1; Bach et al., 2020)
123 in waters 30 m deep. Each individual mesocosm consisted of a cylindrical polyurethane bag (2 m diameter, 18.7 m length,
124 54.4 ± 1.3 m³ volume) suspended in an 8 m tall flotation frame. Water exchange was permitted via nets (mesh size 3mm) for
125 three days before the water mass inside each mesocosm was enclosed and isolated from the surrounding Pacific water by
126 attaching sediment traps at the base (~19 m length total). The enclosing of the mesocosms marked the start (day 0) of the 50-
127 day experiment. As detailed in Bach et al. (2020), the experiment involved several manipulations including the addition of
128 ODZ water to simulate upwelling conditions, salt to maintain water stratification, and the introduction of organisms.
129

130 The collection of subsurface waters and their addition to the mesocosms is described with detail in Bach et al. (2020). Briefly,
131 on experiment days 5 and 10, two batches of local subsurface ODZ water were collected from stations with varying nutrient
132 stoichiometries (Table 1; Fig. 1) using deepwater collectors first reported by Taucher et al., (2017). The water mass collected
133 from 30 m deep at station 1 (12.028323° S, 77.223603° W) was characterized by a very low N:P ratio (Table 1), whereas the
134 water collected from 70 m deep at station 3 (12.044333° S, 77.377583° W) was characterized by a higher but still low N:P
135 ratio (Table 1). On experiment day 8, 9 m³ of water was removed from each mesocosm at a depth between 11 and 12 m and
136 then on day 11, 10 m³ of ODZ water was injected into each mesocosm at depths between 14 and 17 m. On experiment day 12,
137 the entire procedure was repeated but this time with 10 m³ removed between 8 and 9 m, and 12 m³ added evenly between 1
138 and 9 m. To maintain stratification and preserve the low O₂ subsurface layer, a NaCl brine solution was injected evenly into
139 the subsurface of all mesocosms on experiment day 13 (0.067 m³, 10 to 17 m depth) and experiment day 33 (0.046 m³, 12.5 to
140 17 m depth). On day 14, Peruvian Scallop larvae (*Argopecten purpuratus*) were added (~10,000 individuals m⁻³), and on day
141 31 Fine Flounder eggs (*Paralichthys adspersus*) were added (~90 individuals m⁻³). However, few scallop larvae and no fish
142 larvae were found in the mesocosms after the release indicating that their influence on the plankton community was likely
143 small (Bach et al., 2020).
144

145 We sampled two integrated water depths of the mesocosms for suspended organic matter and biological and chemical
146 characterization using 5 L integrating water samplers (IWSs; Hydro-Bios, Kiel) equipped with pressure sensors to collect water
147 evenly within a desired depth range. The samples were collected across two integrated intervals of the water column
148 representing surface and subsurface layers, sampling depths were slightly modified over the course of the experiment to
149 accommodate for changes in water stratification and the position of the chemocline (refer to Bach et al., 2020 for further
150 details). The depths applied for surface and subsurface waters were 0–5 and 5–17 m on days 1 and 2, 0–10 and 10–17 m from
151 day 3 to 28, and 0–12.5 and 12.5–17 m from day 29 to 50.

152
153 Samples of suspended organic matter for IPL analysis were collected from all 8 mesocosms at both the surface and subsurface
154 sampling depths on non-consecutive days throughout the experiment. See details of changes in water depths above. Due to the
155 labor- and time-intensive nature of IPL analysis, we focused on 4 mesocosms (two from each treatment) at both depths and
156 from 9 different days spanning the 50-day experiment. We filtered 5 L of mesocosm water through pre-combusted, 142 mm
157 Advantec glass fiber filters (GF75142MM) of 0.3 μm pore size. All samples were wrapped in combusted aluminum foil and
158 shipped frozen to the Organic Geochemistry Laboratory at the University of Colorado, Boulder for IPL extraction and analysis.

159 **2.2 Water Column Physicochemistry**

160 Depth profiles of salinity, temperature, O_2 concentration, photosynthetically active radiation (PAR), and chlorophyll a (chl-a)
161 fluorescence were measured through vertical casts using the CTD60M sensor system (Sea & Sun Technology). O_2
162 concentrations were cross-verified with the Winkler O_2 titration method performed via a micro-Winkler titration method
163 described by Aristegui and Harrison (2002). Seawater pH_T (pH on total scale), was determined spectrophotometrically using
164 m-cresol purple (mCP) indicator dye as described in Carter, et al. (2013); see Chen et al. (2022) for details. See Bach et al.
165 (2020) for additional detailed information of sampling methods for water column physicochemistry.

166
167 Samples for inorganic nutrients were filtered immediately upon arrival at the laboratories at the Instituto del Mar del Perú
168 (IMARPE) using 0.45 μm Sterivex filter (Merck). The subsequent analysis was carried out using a continuous flow analyzer
169 (QuAAtro AutoAnalyzer, SEAL Analytical) connected to a fluorescence detector (FP-2020, JASCO). The method for
170 analyzing PO_4^{3-} followed the procedure outlined by Murphy and Riley (1962), while $\text{Si}(\text{OH})_4$ was analyzed according to Mullin
171 and Riley (1955). NO_3^- and NO_2^- were quantified through the formation of a pink azo dye as established by Morris and Riley
172 (1963) and additional corrections to all colorimetric methods was achieved with the refractive index method developed by
173 Coverly et al. (2012). Ammonium concentrations were determined fluorometrically following the method of K erouel and
174 Aminot (1997). Further methodological specifics and the respective limits of detection for each analysis can be found in Bach
175 et al. (2020).

176 **2.3 CHEMTAX Analysis**

177 Pigment samples were flash-frozen in liquid nitrogen directly after filtration and kept frozen on dry ice during transport to
178 Germany for extraction as described by Paul et al. (2015). Concentrations of extracted pigments were measured by reverse-
179 phase high-performance liquid chromatography (HPLC; Barlow et al., 1997) calibrated with commercially available standards.
180 The relative contribution of distinct phytoplankton taxa was calculated with CHEMTAX, a program for calculating the
181 taxonomic composition of phytoplankton populations (Mackey et al., 1996). Input pigment ratios specific to the Peruvian
182 upwelling system, determined by DiTullio et al. (2005) and further described by Meyer et al. (2017), were incorporated in
183 these calculations (see Bach et al., 2020).

184 **2.4 Flow Cytometry**

185 Samples (650 μL) from each mesocosm were analyzed using an Accuri C6 (BD Biosciences) flow cytometer. The signal
186 strength of the forward light scatter was used to distinguish phytoplankton groups, in addition to the light emission from red
187 fluorescence of chl-a, and the light emission from orange fluorescence of phycoerythrin. Size ranges were constrained via
188 gravity filtration using sequential polycarbonate filters ranging from 0.2 to 8 μm and the strength of the forward light scatter
189 signal. Additional details of this method can be found in Bach et al., 2017. In this study, we only report *Synechococcus* (0.8-3
190 μm) counts (cells mL^{-1}) because it is the only phytoplankton group that was consistently selected to exhibit statistically
191 significant trends with IPLs likely due to the non-size fractionated nature of IPL sampling.

192 **2.5 Lipid Extraction and Analysis**

193 Intact polar lipids were extracted from glass fiber filters via a modified version (Wörmer et al., 2015) of the original Bligh and
194 Dyer Extraction method (Bligh and Dyer, 1959). Samples were extracted by ultrasonication a total of five times, with three
195 different extraction mixtures. Two extractions were performed using Dichloromethane:Methanol:Phosphate buffer
196 (aq) [1:2:0.8, v:v:v], adjusted to a pH of ~ 7.4 , followed by another two extractions using
197 Dichloromethane:Methanol:Trichloroacetic acid buffer(aq) [1:2:0.8, v:v:v], adjusted to a pH of ~ 2.0 . A final extraction was
198 performed with Dichloromethane:Methanol [1:5, v:v]. After each addition, samples were vortexed for 30 s, sonicated for 10
199 min, and then centrifuged for 10 min at 3000 rpm while kept at 10 $^{\circ}\text{C}$. The supernatant of each extraction mixture was then
200 transferred to a separatory funnel where the organic fractions were washed and combined before solvent removal under a
201 gentle N_2 stream. Before analysis, the TLEs were resuspended in dichloromethane:methanol (9:1 v:v) and filtered through a
202 0.45 μm polytetrafluoroethylene (PTFE) syringe filter.

203
204 Chromatographic separation and identification of IPLs was achieved using a Thermo Scientific UltiMate 3000 high-
205 performance liquid chromatography (HPLC) interphase to a Q Exactive Focus Orbitrap-Quadrupole high resolution mass
206 spectrometer (HPLC-HRMS) via heated electrospray ionization (HESI) in positive mode, as described in detail in applications

207 by Cantarero et al. (2020) and Flores et al. (2022). Briefly, a flowrate of 0.4 ml/min was applied to an Aquity BEH Amide
208 column (150 mm, 2.1 mm, 1.7 μm) using a gradient program first described by Wörmer et al (2013). All filtered TLEs were
209 suspended in Dichloromethane:Methanol (9:1, v/v) prior to injection (10 μL) on column. The following HESI conditions were
210 applied; auxiliary gas temperature: 425 $^{\circ}\text{C}$, capillary temperature 265 $^{\circ}\text{C}$, spray voltage 3.5 kV, sheath gas flow rate: 35
211 arbitrary units (AU), auxiliary gas flow 13 AU, S-Lens RF level 55 AU. Samples were analyzed in full scan mode to obtain
212 an untargeted screening (or lipidomic profile) of each sample, in addition to targeted MS/MS mode for compound identification
213 via diagnostic fragmentation patterns (e.g., Sturt et al., 2004; Schubotz et al., 2009; Wakeham et al., 2012). IPLs were identified
214 by their exact masses, polar head groups, the total number of carbon atoms and unsaturations in the core structure, and their
215 retention times. While other studies have analyzed IPLs under both positive and negative ionization modes to determine the
216 composition of individual fatty acid chains in the core lipid structures, we took advantage of the high resolution of the Orbitrap
217 mass spectrometer to focus on the diversity of head group combinations with total carbon atoms and unsaturation only
218 (Cantarero et al., 2020).

219
220 Quantification of IPLs was achieved using a combination of an internal standard added (2 μg) to samples during extraction
221 (C16 PAF, Avanti Lipids), in addition to an external calibration curve consisting of 17 standards representing different IPL
222 classes (see Cantarero et al., 2020 for full details of all internal/external and deuterated standards). The intensity of each
223 individual IPL identified in the HPLC-HESI-HRMS analysis was calibrated to a linear regression between peak areas and
224 known concentrations of the same lipid class (or the most similar molecular structure) across a 5-point dilution series (0.0001–
225 10 ng/ μl). The detection limit, based on individual calibration curves, was determined to be 0.01 ng on column except for
226 DGTS (0.001 ng) and DG, MG, and SQ classes (0.1 ng). Samples were analyzed across 3 separate analytical periods with
227 weekly calibration curves to account for variation in the ionization efficiency of compounds over time. Overall, HPLC-ESI-
228 HRMS is considered a semi-quantitative method due to changes in ionization efficiency of different IPL standards and
229 environmental analytes. These changes are largely caused by differences in polar head group compared to the acyl chain length
230 and degree of unsaturation (Yang and Han, 2011). Nonetheless, we investigate both relative (%) and absolute IPL abundances
231 to compensate for the current analytical limitations in IPL quantification.

232
233 While we report IPL structural variations associated with different head groups and modifications in the core structure (i.e.,
234 unsaturation degree and carbon length of diacyl chains), we particularly focus on the former. Additionally, several IPLs thought
235 to be absent in eukaryotic phytoplankton or far more abundant in bacteria and archaea ($n = 34$ in total) have been removed to
236 facilitate the analysis of trends that are predominantly phytoplanktonic in origin. These compounds include PME/PDME
237 (Phosphatidyl(di)methylethanolamine) and intact GDGTs (glycerol dialkyl glycerol tetraethers) classes. In addition, while we
238 lack detailed structural information of core individual fatty acids, their combined carbon atoms can be used to deduce short
239 (i.e. < 14 carbon atoms per chain) or odd numbered fatty acid chains typically found in bacteria (Volkman et al., 1989; Volkman
240 et al., 1998; Russell and Nichols, 1999; Jónasdóttir, 2019). Thus, compounds conventionally regarded as bacterial (34 in total)

241 were also removed to minimize their impact on the analysis of predominantly phytoplanktonic IPLs (165 in total). We
242 recognize that while this selection approach reduces the influence of non-eukaryotic lipids, we still cannot rule out an
243 undetermined contribution from heterotrophic bacteria to the IPL pool in this experiment. A summary of these IPL classes and
244 their acronyms is provided in Table 2.

245

246 **2.6 Multiple Linear Regression**

247 We performed multiple linear regression between 8 relevant environmental factors and 165 unique IPLs. With so many IPL-
248 environmental factor pairs to analyze, we used multiple linear regression (MLR) for quick and easily digestible outputs. In
249 each MLR model, the relative abundance of individual IPL molecules was employed as a response variable, with environmental
250 factors serving as predictor variables. Additionally, phytoplankton abundances were included to account for their linear effects
251 on IPL distributions. The rationale behind this inclusion lies in the understanding that variations in phytoplankton abundance
252 may exert a proportional and predictable impact on the abundance patterns of specific IPLs.

253

254 We prioritized linear relationships with IPL relative abundances (% abundances) to emphasize changes in the proportions of
255 phytoplankton lipids, rather than their absolute concentration and contribution to biomass. This approach enables us to
256 distinguish compositional changes in the lipid pool from variability in total biomass production. Additionally, MLRs were
257 constrained to focus on the most abundant IPLs in this system, defined as those constituting more than 2.5% to the total IPL
258 pool. This restriction was implemented to reduce noise associated with low-abundance IPLs and enhance the robustness of
259 analysis.

260

261 We chose to investigate linear relationships within individual depths (surface and subsurface) to focus on temporal changes
262 within distinct environments, rather than comparing these two environments directly (see CART and Random Forest methods,
263 below). IPLs and environmental factors were permuted to tabulate the regression coefficient for each IPL-environmental factor
264 pair. Model coefficients were directly comparable due to centering and scaling of environmental and phytoplankton variables
265 (see eq. 1) to linearize the relationship and better align with the model assumptions:

266

$$267 \quad Y = \beta_0 + \beta_1 X_1 + \beta_2 X_2 + \dots + \beta_n X_n + \varepsilon \quad \text{eq. (1)}$$

268 where, Y is the dependent variable (or response), X_1, X_2, \dots, X_n are the predictor variable (or independent variables), β_0 is the
269 intercept (constant term), $\beta_1, \beta_2, \dots, \beta_n$ are the coefficients representing the magnitude and direction of the relationship between
270 the predictor variable and the dependent variable, and ε is the error term capturing the variability not explained by the model.

271 Correlations in the MLR analysis were also controlled for false discovery rate following the procedure of Benjamini and
272 Hochberg, (1995) to calculate adjusted p-values and by applying an alpha cutoff of 0.1.

273

274 **2.7 Classification and Regression Tree (CART) and Random Forest**

275 Classification and Regression Trees (CART; Breiman et al., 1984) are predictive machine learning algorithms that partition
276 and fit data along a predictor axis into homogenous subsets of the dependent variable. Regression trees are used for dependent
277 variables with continuous values, while classification trees for categorical values. Here, we apply regression trees to diagnose
278 the environmental and biological variables that affect IPL concentrations by polar head group class. We limited the size of the
279 tree splits via a “pruning” process, where less significant variable splits are removed as determined by a deviance criterion
280 resulting in the best-fit tree with the least mean squared error. Additionally, predictor variables were selected in conjunction
281 with random forest analyses, which ranks the variable contribution to the model performance.

282

283 Random forests are derived from bootstrapping of observational data, and the generation of many decision trees based on each
284 bootstrap sample. We employed a total of 72 samples for the random forest analysis which was run separately for each major
285 IPL class ($n = 7$) to identify the most important environmental predictors ($n = 12$) for each individual class of lipid. The random
286 forest method utilizes bootstrap aggregation to generate and average numerous permutations of an out-of-bag score in
287 predictive performance. This approach offers an effective methodology for analyzing high-dimensional data with limited
288 sample sizes (Biau and Scornet, 2016). This method has been widely adopted across various disciplines within the water
289 sciences (Tyrallis, 2019), ecological and species distribution modeling (Luan et al., 2020), as well as in bioinformatics and
290 high-throughput genomics (Chen and Ishwaran, 2012; Boulesteix et al., 2012). For a covariate vector, the predicted estimate
291 of IPL class concentrations is an average of the many randomly configured decision trees with the same distribution. A
292 randomly generated subset of decision trees is used to split each node, enabling reduced variance and correlation amongst
293 individual trees, and ideally improving the accuracy of model predictions (Breiman, 2001). The random forest algorithm also
294 allows for the ranking of predictor variables based on the prediction performance and is reported here as the predictor’s
295 contribution in reducing the root mean square error (RMSE) in the model. For additional details on the random forest algorithm,
296 please see Hastie et al. (2009). All CHEMTAX, flow cytometry, and physicochemical variables were included in the CART
297 and random forest analyses as predictors. Regression tree (CART) splitting criteria are determined by evaluating the sum of
298 squared deviations in all possible splits and selecting those that result in the greatest reduction of residual error. To prevent
299 overfitting in the CART analysis, a pruning procedure is run to remove nodes that contribute little to the model accuracy based
300 on a cost complexity measure. This procedure allows us to simplify the CART results and thus focus our interpretations on the
301 most significant predictors of IPL headgroups only. In the Random Forest model, following the averaged cross validated
302 accuracy estimates, we implemented a cutoff of 5% reduction in RMSE to eliminate variables that do not significantly reduce

303 the error of the model prediction. This cutoff allows us to focus our interpretation of only variables that contribute significantly
304 to the out of bag predictor performance (For further details, refer to Supplementary Material, Note S1).
305 CART and random forest-based predictions serve as ideal methods to explore environmental drivers of IPL distributions- not
306 only because of their predictive performance- but also because of their non-parametric nature, their diagnosis of variable
307 importance, and their ability to handle non-linear interactions and small sample sizes (Tyralis et al., 2019). We do not employ
308 these methods to predict the concentration of IPL classes, but rather to identify the primary environmental and biological
309 drivers of change in IPL class concentrations, and potential interactions between environmental conditions and IPL remodeling
310 amongst phytoplankton. Therefore, we focus our interpretations of both the CART and Random Forest analyses on only the
311 most significant predictors and their relative order of importance in the model predictions.

312 **3 Results**

313 **3.1 Oxygen and pH_T**

314 Oxygen concentration in surface waters ranged between ~125 and 140 $\mu\text{mol/L}$ before the ODZ water addition in all 4
315 mesocosms (Fig. 2A). The concentration dropped slightly (~15 $\mu\text{mol/L}$) following the water addition and steadily increased
316 to a maximum between ~185-220 $\mu\text{mol/L}$ by day 28. Day 30 marked a significant drop in oxygen concentration by 30-60
317 $\mu\text{mol/L}$ in all mesocosms with conditions stabilizing between 140 and 155 $\mu\text{mol/L}$ by day 50. The temporal variability in pH_T
318 in surface waters showed a largely mirrored trend to that of oxygen content. Before ODZ water addition pH_T was 7.9-8.0,
319 which dropped by ~0.2 immediately following the water addition. After a few days of relatively stable pH_T at ~7.8 in all four
320 mesocosms, the pH_T increased significantly between days 18 and 28 reaching ~8.1-8.2. From days 30-40 the pH_T gradually
321 decreased by approximately 0.2 in all mesocosms until increasing again (most notably in mesocosms 7 and 5) between days
322 42-50 to maxima ranging from 8.1-8.3.

323

324 The subsurface waters were more oxygen-depleted compared to the surface and showed an earlier onset of increasing oxygen
325 concentration, beginning immediately after the ODZ water addition. All four mesocosms reached maximum O₂ levels (60-75
326 $\mu\text{mol/L}$) by day 13 and began decreasing markedly by day 16. The lowest concentrations (~15 $\mu\text{mol/L}$ O₂) were reached
327 between days 30 and 34. Oxygen concentrations recovered slightly in the last 10-16 days of the experiment and were all within
328 30 (\pm 10) $\mu\text{mol/L}$ of O₂. The subsurface waters, again, showed similar temporal patterns in pH_T as with O₂, except for
329 mesocosm 7. The pH_T was variable (~7.60 \pm 0.05) in the early portion of the experiment (days 10-16) but did not show a
330 dramatic response to the OMZ water addition as was the case in the surface samples. The pH_T did gradually decrease from
331 days 18-30, with pH_T minima in all four mesocosms reached on day 30 (~7.45-7.50). Day 30 also marked the beginning of a
332 significant increase in the pH_T (~0.15-0.20) across all mesocosms with the pH_T steadily increasing to ~7.65-7.70 by day 50.
333 Additional details on the carbonate chemistry of the mesocosms can be found in Chen et al. (2022).

334

335 3.2 Nutrient Concentrations

336 In mesocosm surface waters, the nutrients NH_4^+ , NO_3^- , NO_2^- , PO_4^{3-} , and $\text{Si}(\text{OH})_4$ all showed consistent trends over time, with
337 the highest concentrations occurring either just before (day 10) or immediately after (day 12) the ODZ water addition (Fig.
338 2B). Nitrogen species ranged between 1 and 3 $\mu\text{mol/L}$ during this early part of the experiment, while $\text{Si}(\text{OH})_4$ ranged between
339 4 and 7 $\mu\text{mol/L}$, and PO_4^{3-} remained at $\sim 2 \mu\text{mol/L}$. The concentration of all nitrogen species dropped quickly to near minimum
340 values by day 15, and typically remained $<0.5 \mu\text{mol/L}$ for the remainder of the experiment. PO_4^{3-} remained replete (>1.5
341 $\mu\text{mol/L}$ for the entirety of the experiment). $\text{Si}(\text{OH})_4$ dropped to $\sim 3\text{-}4 \mu\text{mol/L}$ by day 15 and gradually increased in all 4
342 mesocosms by 1-2 $\mu\text{mol/L}$ until days 36-38, where concentrations gradually dropped to near minimum values of 3-4 $\mu\text{mol/L}$.
343 There were periodic enrichments in NH_4^+ , most notably between days 40-50, as discussed in Bach et al., 2020.

344
345 The mesocosm subsurface water nutrients showed similar temporal patterns as the surface but were generally more enriched
346 in all nutrient species. All nitrogen species decreased in the few days following the ODZ water addition, but at a more gradual
347 pace than in the surface. Before and immediately after the water addition, NO_3^- was enriched at 4-6 $\mu\text{mol/L}$ and NH_4^+ between
348 2.5-4 $\mu\text{mol/L}$. NO_2^- concentrations were $\sim 0.5\text{-}1 \mu\text{mol/L}$ in mesocosms 6 and 7 during this period but remained low (<0.3
349 $\mu\text{mol/L}$) in mesocosms 5 and 8. Broadly speaking, the nitrogen species all reached minimal values ($<0.1 \mu\text{mol/L}$) by days 18-
350 20, except for in mesocosms 6 and 8, where NO_3^- persisted at significant concentrations (0.2-2.3 $\mu\text{mol/L}$) until days 22 and
351 24, respectively. The remainder of the experiment was marked by typically depleted concentrations of all nitrogen species
352 ($<0.1 \mu\text{mol/L}$) with occasional spikes in NH_4^+ reaching up to 1 $\mu\text{mol/L}$, particularly towards the end of the experiment.
353 Subsurface PO_4^{3-} concentrations were similar to the surface, remaining around $\sim 2.0 \mu\text{mol/L}$ for most of the experiment which
354 gradually decreased to concentrations of $\sim 1.5 \mu\text{mol/L}$ by the end of the experiment. $\text{Si}(\text{OH})_4$ similarly decreased from
355 maximum concentrations of 4.0-4.5 $\mu\text{mol/L}$ shortly after the ODZ water addition, and gradually decreased by $\sim 1 \mu\text{mol/L}$ over
356 the course of the experiment.

357 3.3 Total Chlorophyll a

358 Chl-a concentrations were highly variable throughout the experiment, particularly in subsurface waters (Fig. 2C).
359 Concentrations were generally more elevated at the surface compared to the subsurface, with values ranging $\sim 2.56\text{-}2.96 \mu\text{g/L}$
360 on day 10. In all mesocosms, the chl-a concentration increased to $\sim 7.94\text{-}14.01 \mu\text{g/L}$ after the ODZ water addition and through
361 day 20. Day 22 showed a significant drop in chl-a concentrations to between 1.35 and 2.89 $\mu\text{g/L}$ in mesocosms 7, 5, and 8.
362 Chl-a concentrations at the surface remained rather constant until days 36-40, where concentrations rapidly increased until
363 maximum concentrations on days 48-50 (14.0-47.3 $\mu\text{g/L}$). In subsurface waters, chl-a concentrations were notably lower than
364 in the surface and ranged between 0.58-0.84 $\mu\text{g/L}$ on day 10. After the ODZ water addition, chl-a concentrations increased
365 slightly until day 14, but did not show consistent distributions amongst the 4 mesocosms afterwards; decreases were observed
366 in mesocosms 6, 5, and 8, but an increase in mesocosm 7. Chl-a concentrations increased rapidly on day 22 in all 4 mesocosms

367 ranging between 4.03 and 8.44 $\mu\text{g/L}$. While remaining highly variable, the concentrations generally increased after day 24
368 with a notably abrupt increase between days 40-44 to near maximum values ranging between 2.58-11.3 $\mu\text{g/L}$.

369 **3.4 Phytoplankton Community Composition**

370 The CHEMTAX based phytoplankton community compositions demonstrated more variability in phytoplankton assemblages
371 in the subsurface samples than in the surface (Fig. 2C). Before the ODZ water addition on day 10, surface waters in all 4
372 mesocosms showed similar phytoplankton distributions with high relative abundances of Bacillariophyceae, referred to from
373 here on as diatoms (20-45%), Chlorophyceae (15-50%), and Dinophyceae, referred to as dinoflagellates (25-45%). These
374 distributions remained rather similar immediately after the water addition (day 12), but dinoflagellate contributions increased
375 in the following days and ranged from ~20% of the total chl-a pool to up to 75% by day 20. Of note, Cryptophyceae made
376 minor contributions to the chl-a pool aside from days 15-18 in mesocosm 6 where they contributed up to 25%. Dinoflagellates
377 largely dominated the chl-a pool for the remainder of the experiment with moderate blooms of diatoms between days 34-44 in
378 mesocosms 7 and 8.

379
380 Subsurface waters exhibited greater variability in the phytoplankton assemblages and a greater contribution of Chlorophyceae,
381 Cryptophyceae, *Synechococcus*, and diatoms to the chl-a pool than in the surface. Pre-addition waters (day 10) were dominated
382 by diatoms making up >75% of the chl-a pool. In the first few days after the ODZ water addition (days 12-15), the relative
383 abundance of Chlorophyceae increased to 25-45% in mesocosms 6, 5 and 8, whereas Cryptophyceae contributed between 5-
384 15% of the total chl-a. During this period, diatoms continued to dominate mesocosm 7 but decreased gradually from 65 to 15%
385 of the phytoplankton community. Notably, in mesocosm 6, Cryptophyceae contributed a moderate amount to the chl-a pool
386 beginning on day 15 (25%) and gradually increased to 40% by day 20. Mesocosms 7, 5, and 8 increased in Cryptophyceae as
387 well, but were limited to ~10-25%. Similar to surface waters, dinoflagellates dominated the chl-a pool by day 20 and
388 contributed 50-80% of the chl-a pool; however, there was considerably greater variability in dinoflagellate abundance after
389 day 20 in subsurface waters. Chlorophyceae remained a significant contributor for the rest of the experiment typically ranging
390 between 10 and 25% of the phytoplankton relative abundance. In mesocosms 7, 5, and 8 diatoms became the dominant
391 contributor, totaling ~50% of the phytoplankton between days 32 and 44. By the final days of the experiment (days 48-50),
392 dinoflagellates again made up most of the phytoplankton community (60-75%). Pelagophyceae, Prymnesiophyceae, and
393 Cyanophyceae (referred to here as *Synechococcus*), remained minor contributors throughout the entire experiment but showed
394 maximum contributions of <10% in days 10-16. Mesocosm 6 showed a minor contribution (<10%) of *Synechococcus* from
395 days 42-50, and from days 34-42 in mesocosm 7.

396 **3.5 IPL Class Distributions**

397 The IPL distributions throughout the study can be summarized by the relative abundances of different classes determined by
398 their polar head groups. IPL distributions were broadly consistent between mesocosms and treatments during the experiment

399 but showed significant differences between surface and subsurface waters (Fig. 2D). Glycolipids such as SQ, DG, and MG
400 typically made up ~50-75% of the total IPL pool in the surface, whereas phospholipids such as PC and PG were dominant in
401 the subsurface (~50-75%). The changes in IPL distribution from the surface samples over the course of the experiment were
402 most apparent between days 10 to 12, 20 to 24, and 24 to 38. Day 10 of the experiment marks the sampling period immediately
403 preceding the ODZ water addition and was the only day with a significant fraction of BLs (betaine lipids) in the total lipid
404 pool (ranging from 25-30% in the surface samples). Mesocosms 6 and 8 showed a similar distribution between days 10 and
405 12 of the experiment with large contributions of SQs (~50%), BLs (~25-30%), and MGs (~20%), while mesocosms 7 and 5
406 showed considerably more PCs (~25-40%) at the expense of SQs (<10%). In the 2 weeks following the deep-water addition
407 (days 12 to 24), we saw increasing (albeit variable) relative abundances of PGs (from 5 to 50%) and DGs (from 5 to 25%) in
408 surface waters. MGs made up a considerably larger fraction during this time in mesocosm 6 (up to 50%), but were more
409 moderate in mesocosms 7, 5, and 8 (typically ~25%), yet decreased in all mesocosms to <5% by day 24. The final sample days
410 (38 and 50) showed a resurgence of glycolipid contributions, namely in SQs (25-55%) and MGs (5-25%), with moderate
411 contributions of PGs (5-20%) and DGs (5-20%).

412

413 In the subsurface samples before the ODZ water addition, mesocosms 6, 7, and 8 showed moderate contributions of MGs (15-
414 25%) which was lower in mesocosm 5 (<5%). There were higher contributions of SQs in mesocosms 6 and 8 (50% and 35%,
415 respectively) than in 7 and 5 (20-25%). Instead, mesocosms 7 and 5 showed a greater contribution of PCs (45-55%). All 4
416 mesocosms demonstrated some component of PGs ranging from 5-20% of the total IPL pool. The 2 weeks following the ODZ
417 water addition showed highly variable fluctuations between PCs and PGs as the dominant IPL classes, with the contributions
418 of glycolipids (25-40%) and betaine lipids (<5%) remaining consistent. Of note, day 24 marked a consistently low contribution
419 of PCs, which persisted until the end of the experiment. The final sample days (38 and 50) showed similar contributions
420 between MGs, SQs, and PGs that together dominated the total lipid pool.

421 **3.6 Multiple Linear Regressions**

422 We found statistically significant ($p < 0.05$) linear relationships between the relative abundance of individual IPLs and
423 environmental factors (Figure 3). In surface waters, pH_T showed several significant responses towards DGs, MGs, PGs, PEs
424 and SQs. Classes DG, MG, PE and PG showed negative linear relationships with pH_T . SQs (specifically SQ-32:0), however,
425 showed a strong positive linear response to pH_T . In the subsurface, pH_T only imparted significant linear effects towards SQs
426 with a strong negative linear correlation.

427

428 The temperature of surface waters showed predominantly positive regression coefficients with several PG, MG, and DG
429 molecules, with inconsistent correlations found in SQs. Whereas some PEs showed significant linear relationships with
430 temperature, their regression coefficients were near 0. Similarly, in the subsurface only 1 IPL structures (SQ 34:3) showed a
431 significant positive linear response but with a regression coefficient near 0.

432

433 Oxygen concentrations showed few linear correlations at the surface and were limited to two BLs (negative) and 1 PG
434 (positive). In the subsurface, the strongest linear correlations were found between oxygen and PGs and SQs (negative).

435

436 Nutrient concentrations showed many significant linear responses with regression coefficients of higher magnitude (up to ± 8)
437 and adjusted R^2 values of up to 0.5. The concentration of various forms of inorganic nitrogen had largely positive linear
438 responses to BLs and PCs in both the surface and subsurface, with strongly negative responses in PGs and subsurface MGs .
439 Among the SQs, many individual molecular species, with different fatty acid chains, responded linearly to all forms of
440 inorganic N, the signs of these relationships were negative but in the surface, and generally positive in the subsurface (aside
441 from NO_2^-). DGs showed only one positive linear response in the subsurface. PEs showed little response to inorganic nitrogen
442 concentrations (regression coefficients near 0). PO_4^{3-} concentrations showed only a few significant responses from BLs
443 (negative) and PGs (slightly positive) in the surface. However, in the subsurface, PO_4^{3-} showed strong linear responses
444 (negative) to several MG and PG molecules, and strong positive relationships with several PCs.

445

446 Light showed few linear responses amongst IPL relative abundances. At the surface, the strongest relationships were amongst
447 PG (positive) and SQ (mixed signs) and to a slight degree BLs (negative). In the subsurface, only one SQ with a significant
448 linear relationship was noted and with a weak regression coefficient, indicating a range of light saturation with little to no
449 linear effect on IPL distributions.

450

451 **3.7 CART and Random Forest**

452 All the predictive tree-based models showed improved performance with the inclusion of environmental variables (Figs. 4-7).
453 The CART decision trees iteratively identified the key biological and physicochemical variables producing the best performing
454 model in the prediction of IPL concentrations. The random forest analysis compliments these best fit decision trees by
455 calculating the % reduction in the root mean square error (RMSE) associated with each variable. In conjunction, these two
456 analyses highlight the most impactful variables in predicting the concentrations of a given IPL class. Overall, model
457 performance amongst each IPL class can be compared by the strength of the correlation coefficients between observed and
458 predicted concentrations, and by the magnitude of the RMSE (Figs. 4-7).

459

460 Amongst several IPL classes (i.e., SQs, DGs, and BLs), pH_T was consistently a significant contributing variable to IPL
461 concentrations, as demonstrated by both the CART and random forest analyses (Fig. 4A-D, and Fig. 5). Notably, pH_T was
462 identified as the most important variable amongst the best fit decision trees for both SQs and DGs, as well as the random forest
463 model for SQs. Oxygen concentration was also frequently identified as a major contributing variable to model performance
464 with MGs, DGs, PEs, PCs, (Figs. 4E-H, 5A-D, 6E-H, and 7A-D, respectively) and moderately important in SQs (Fig. 4A-D).

465 Temperature was selected as the most important variable in PE predictions (Fig. 6E-H), and a major contributing variable in
466 SQ, MG, BL, PG, and PC predictions (Figs. 4-7). Various forms of biologically available nitrogen were also important in the
467 prediction of MG (Figs. 4E-H), BLs (NH_4^+ ; Figs. 5E-H), PE (NH_4^+ ; Figs. 6E-H), and PG (NH_4^+ and NO_2^- ; Figs. 6A-D). PO_4^{3-}
468 concentrations showed significant contribution to model performance amongst BLs (Figs. 5E-H, denoted as Si:P ratios), SQs,
469 MGs, PGs, and PEs (Figs. 4A-D, 4E-H, 6A-D, and 6E-H, respectively). Finally, light availability demonstrated secondary but
470 significant importance in the prediction of SQs, MGs, PGs, PEs, and PCs (Figs., 4A-D, 4E-H, 6A-D, 6E-H, and 7 respectively).

471

472 Variables indicative of biological abundance were also identified as highly impactful to model performance, with chl-a
473 concentration showing a significant contribution to all lipid classes except BLs (Figs. 4-7). Individual phytoplankton
474 abundances also showed to be important predictive variables such as Cryptophyceae abundances for BLs, dinoflagellate
475 abundances for DGs and SQs, *Synechococcus* abundances for DGs, PCs, PEs, and PGs, and diatoms for PCs.

476 **3.8 Water Treatments**

477 The experiment consisted of applying two different treatments to the mesocosms, aimed at exploring the varying impacts of
478 upwelling of ODZ waters with contrasting geochemical properties. The first treatment saw the introduction of water from a
479 coastal area (station 1) with ODZ waters with a very low N:P ratio (0.1; see Table 1, and Fig 2B) into the mesocosm. The
480 second treatment performed the same process, but with ODZ water from an offshore area (station 3) with a low N:P ratio (1.7;
481 Table 1, and Fig 2B). Despite the different chemical signatures of the added water-masses, the resulting nutrient stoichiometries
482 within the mesocosms were similar in between both treatments, likely due to both dilution effects and the time passed between
483 water collection and addition (see Bach et al., 2020). We see largely similar responses in the IPL distributions, as well as in
484 other biogeochemical variables between these two treatments; therefore, we largely focus our discussion on the temporal
485 variation and differences between surface and subsurface environments in these analyses.

486 **4 Discussion**

487 **4.1 Biological Abundances as Drivers of IPL Distributions**

488 We expect phytoplankton abundances to exert first order control on the production and distribution of IPLs in this experiment.
489 The majority of the detected molecules have been demonstrated to be chemotaxonomic biomarkers of planktonic biomass
490 (Sturt et al., 2004, Schubotz et al., 2009, Wakeham et al., 2012; Van Mooy and Fredricks, 2010; Cantarero et al., 2020).
491 Previous work in the Humboldt Current System shows that the ratio of total IPLs to POC is high at the chlorophyll maximum
492 and the composition of IPLs found in these surface waters are consistent with predominantly phytoplanktonic biomass
493 (Cantarero et al., 2020). In this mesocosm experiment, the depths of the chlorophyll maximum and oxycline are compressed
494 into a 20 m water column which likely drives a greater contribution of phytoplanktonic IPLs in ODZ waters than would be
495 expected in the natural environment. While we suggest that most of the biomass (and IPL content) measured at these high

496 chlorophyll depths is likely derived from phytoplankton, we cannot completely isolate nor quantify the contribution of bacterial
497 biomass to the total IPL pool.

498
499 Most IPL classes demonstrate phytoplankton abundances as a primary or major predictor in the CART and random forest
500 analyses, such as dinoflagellates in the prediction of SQs (Figs. 4A, C), DGs (Figs. 5A, C), and PE (Fig. 6G), *Synechococcus*
501 in the prediction of PGs (Fig. 6A, C), PEs (Fig. 6E, G), and PCs (Fig. 7A, C), and chl-a in the prediction of every IPL class
502 barring BLs (a mostly minor IPL class in this experiment). Chl-a appears most important in highly abundant IPL classes as an
503 indicator of overall photosynthetic productivity, and dinoflagellates dominate the overall phytoplankton biomass for almost
504 the entirety of the experiment post ODZ water addition. *Synechococcus* demonstrates covariance with the total phytoplankton
505 biomass, yet remains a relatively minor phytoplankton class. We suggest that the prevalence of biological sources as IPL
506 predictors in the decision tree analyses generally indicates the variability in total phytoplankton biomass throughout the
507 experiment.

508
509 Among phytoplankton, glycolipids MG, DG, and SQ are predominantly found in thylakoid membranes, whereas phospholipids
510 PC and PE, as well as BLs are structural components in the cell membrane lipid bilayer (note PG is found in both; Guschina
511 and Harwood, 2013). It is important to recognize that the relative proportions of IPLs vary in different phytoplankton classes
512 (Harwood and Jones, 1989; Wada and Murata, 2009), and that many of these lipids, in particular phospholipids, can also be
513 derived from heterotrophic bacterial biomass (Popendorf et al., 2011). Thus, the overall community composition is expected
514 to be a major driver of IPL distributions in this system. However, given the prevalence of algal biomass and the steps taken to
515 minimize bacterial contributions to the IPL pool (see section 2.5), we focus our analysis on that of phytoplanktonic dynamics.
516 We recognize that both phytoplankton abundances and the total planktonic community composition play a major role in the
517 distribution of IPLs. Thus, while the data presented here may refine the phylogenetic association between biological sources
518 and IPLs in marine systems, our main aim is to explore the role of multiple environmental forcing as an additional control on
519 IPL distributions. The following sections focus on the evidence for direct environmental influence on IPL remodeling amongst
520 the phytoplankton community and the potential implications of these physiological responses to broader aspects of ocean
521 biogeochemistry.

522 **4.2 Environmental Variables as Drivers of IPL Remodeling**

523 Since community composition can change concurrently and/or in response to environmental conditions, we employed two
524 distinct strategies to isolate the role of lipid remodeling as a physiological response to environmental forcing only. Firstly, the
525 MLRs which subtract the variability explained by phytoplankton abundance (e.g., CHEMTAX results) in pairwise correlations
526 between lipid abundances and environmental variables. Secondly, the decision tree analyses (CART and Random Forest)
527 which rank variables by their impacts on the model performance.

528

529 Across virtually every major IPL class common to eukaryotic phytoplankton we see evidence of environmental conditions
530 exerting significant control on polar headgroup distributions in the MLRs (Fig. 3). Similarly, nutrient concentrations, pH_T,
531 temperature, O₂ concentration, and light availability are consistently identified as statistically important variables in the
532 prediction of IPL head groups in both the CART and Random Forest analyses (Figs. 4-7). In addition, high level comparisons
533 in the relative abundances of IPLs and phytoplankton groups (Figs. 3C, D) suggest that certain environmental conditions may
534 be associated with major shifts in IPL distributions.

535

536 An important distinction between the MLRs and the decision trees is that the MLRs are calculated within individual depth
537 environments (surface and subsurface) to explore statistically significant linear relationships between abundant IPL molecules
538 and changing environmental conditions. On the other hand, the decision trees explore the predictive power of physicochemical
539 differences between the surface and subsurface environments on IPL distributions. The results of these two analyses are meant
540 to be complimentary, in that they focus on the differences in environmental conditions between water depths as well as the
541 temporal development of conditions within a given depth over the course of the experiment.

542 **4.2.1 Nutrient Availability**

543 Nutrient limitation amongst phytoplankton leads to transitions in cellular activity, from the biosynthesis of
544 growth/reproduction cellular components such as cell membranes to energy storing molecules (Guschina and Harwood, 2013,
545 Zienkiewicz et al., 2016). Nitrogen, an essential nutrient in photosynthesis and the biosynthesis of proteins/enzymes and
546 nucleic acids, is typically acquired by marine phytoplankton through inorganic nitrogen species such as NO₃⁻ and NH₄⁺. Some
547 phytoplankton can also utilize organic nitrogen sources (Bronk et al., 2007), whereas diazotrophic cyanobacteria can fix
548 dinitrogen gas into bioavailable nitrogen. The coastal region of the ETSP is typically considered to be seasonally co-limited
549 by light, N, and Fe (Messié and Chavez, 2015). However, along the Peruvian shelf Fe concentrations are elevated compared
550 to offshore waters (Hutchins et al., 2002; Browning et al., 2018), and is not considered a limiting source in this mesocosm
551 experiment (Bach et al., 2020). In our mesocosm systems, the inorganic N:P ratio ranged between 0.13 and 4.67, with higher
552 inorganic N in subsurface waters compared to the surface, and with a N:P minimum reached by day 20. Bach et al., (2020)
553 noted that a week after the ODZ water addition, increases in the particulate organic carbon to biogenic silica ratios coincided
554 with low inorganic N and high Si(OH)₄ concentrations, suggesting a N-limited system. Thus, we consider our system to be
555 overall nitrogen limited with varying degrees of severity throughout the course of the experiment. This N-limitation is also
556 reflected in the transition from predominantly diatoms, Chlorophyceae, and Cryptophyceae to a dominance of mixotrophic
557 dinoflagellates approximately 4-6 days after the initial ODZ water treatment (Bach et al., 2020). Such shifts are consistent with
558 the ecological advantage that dinoflagellates exhibit under N-limiting conditions as they can extract nitrogen from the dissolved
559 organic nitrogen (DON) pool (Kudela et al., 2010) as well as from heterotrophy (Smalley et al., 2003).

560

561 In our study, all four mesocosms experienced limitations in inorganic nitrogen (as low as 0.24 $\mu\text{mol/L}$) and consistently high
562 concentrations of PO_4^{3-} (ranging from 1.3 to 2.3 $\mu\text{mol/L}$) throughout the entire experiment. Random forest analysis shows that
563 the inorganic N concentration is an important predictor in the abundance of BL, PG, and MG (Figs. 5G, 6A, and 4E,
564 respectively). The MLRs also indicate that many individual molecules from nearly every IPL headgroup have significant linear
565 correlations with inorganic N concentrations (Fig. 3). Of note, the distributions of several abundant PCs and BLs with N in the
566 headgroup structure are consistently positively correlated with inorganic N species. Whereas other non-N-bearing IPLs are
567 generally negatively correlated with inorganic N concentration (PG, SQ and MG) meaning that they are proportionally more
568 abundant under more severe N-limitation.

569

570 Under P limitation, phytoplankton are known to substitute non-phosphorus-containing glycolipids for phospholipids and
571 reallocate the liberated P for other cellular demands (Van Mooy et al., 2009). We hypothesize that non-N-containing
572 glycolipids and phospholipids may similarly be substituted for IPLs such as PCs and BLs as a mechanism for alleviating
573 cellular N demand in low inorganic N conditions. Both PC and BL are found in extra-chloroplast membranes (Kumari et al.,
574 2013), whereas IPLs found in thylakoid membranes such as MG, PG, and SQ are essential to the photosynthetic machinery.
575 Indeed, the average ratio of total IPLs/chl-a is up to three times higher at depth than in surface waters (Fig. S5), possibly
576 pointing towards a reduced proportion of membrane lipids among phytoplankton subject to environmental stressors such as
577 nutrient limitation (likely in addition to oxygen availability, temperature, and light levels). We note that at least a fraction of
578 this trend could also be explained by the contribution of IPLs from heterotrophic bacteria.

579

580 More generally, nutrient limitation can cause phytoplankton to accumulate highly concentrated stores of energy in the form of
581 triacylglycerols (TAGs) through the activation of multiple biosynthetic pathways (Zienkiewicz et al., 2016). These include
582 synthesis via acyl units donated from phospholipids via the PDAT (phospholipid:diacylglyceroltransferase) enzyme (Dahlqvist
583 et al., 2000), or other chloroplast membranes, as demonstrated in the homologous enzyme Cr-PDAT (Yoon et al., 2012), as
584 well as several DGAT(diacylglycerol:acyl-CoA acyltransferases; Li et al., 2012; Li-Beisson et al., 2019). These enzymes
585 represent significant pathways for TAG accumulation (Popko et al., 2016; Gu et al., 2021), are sensitive to N availability
586 (Yoon et al., 2012; Li et al., 2012), and their encoding genes have so far been identified in green algae, diatoms, and heterokonts
587 (Zienkiewicz et al. 2016). Because our dataset does not include TAG production, further work on this aspect could reveal
588 whether the proportional changes in dominant phytoplanktonic IPLs correlated to N availability are also associated with TAG
589 synthesis, and if so, determine whether recycling of membrane lipids is a significant contributor to these observed community-
590 level distributions.

591

592

593 4.2.2 pH_T and Inorganic Carbon Availability

594 Coastal upwelling zones are characterized by low pH_T subsurface waters associated with ODZs, where high fluxes of organic
595 substrates sustain enhanced microbial respiration and the accumulation of CO₂ (Capone and Hutchins, 2013). Thus, we explore
596 evidence for membrane lipid remodeling amongst phytoplankton as a physiological response to varying pH_T. We see evidence
597 of pH_T imparting a potential control on the composition of IPL head groups, particularly amongst SQs and DGs, as noted by
598 the high importance rankings in both the CART and Random Forest analyses (Figs. 4A,C and 5A,C). This likely represents
599 the relatively high abundance of these glycolipids in the surface samples where the pH_T is 0.2-0.6 higher than at depth. The
600 MLRs show several negative correlations between MG, PG, and SQ molecules containing unsaturated or polyunsaturated fatty
601 acids with pH_T (Fig. 3). The observed increased proportion of unsaturated IPLs at lower pH_T is most apparent in surface waters
602 where the variability in pH_T is greatest (± 0.2). It has been suggested that lower pH_T can induce greater proportions of saturated
603 fatty acids as a mechanism to reduce membrane fluidity and prevent high proton concentrations in the cytoplasm (Tatsuzawa
604 et al., 1996). However, this response remains limited to more extreme pH_T ranges (e.g., ~1-10), suggesting that other
605 environmental factors (e.g. nutrient availability) are overprinting the potential impacts of pH on fatty acid saturation.

606
607 Rather than a direct consequence of modest changes in pH_T on algal membrane fluidity, the observed changes in fatty acid
608 profiles may be in part a response to the available forms of inorganic carbon for photosynthesis. Following the ODZ water
609 addition, DIC (dissolved inorganic carbon) and pCO₂ rapidly declined within a few days (Chen et al., 2022) due to high
610 productivity. In natural waters, pCO₂ maxima occur in ODZ waters where respiration rates are high (Vargas et al., 2021).
611 Lower pCO₂ at the surface may be a limiting factor for photosynthesis and growth; higher pH_T in marine settings indicates a
612 reliance on active transport of HCO₃⁻ for carbon fixation as opposed to a passive diffusion of CO₂ (Azov et al., 1982; Moazami-
613 Goudarzi et al., 2012). Enrichment of pCO₂ has also been observed to induce an increased proportion of unsaturated fatty acids
614 in microalgae (Morales et al., 2021), which may explain the negative correlation between the proportion of certain unsaturated
615 glycolipids (as well as PGs) and pH_T (high pCO₂; see Fig. 3).

616
617 As mentioned above, phytoplankton can employ membrane lipids as substrates for TAG accumulation in phytoplankton under
618 environmental stress. While nutrient limitation is often considered the primary regulator of TAG production, culture
619 experiments also point toward the importance of pH and inorganic carbon availability (Guckert and Cooksey, 1990; Gardner
620 et al., 2011), with different responses between a model diatom (*Phaeodactylum tricorutum*) and chlorophytes (CHLOR1 and
621 *Scenedesmus sp.* WC-1), which is potentially related to individual carbon concentrating mechanisms (Gardner et al., 2012).
622 For instance, under nitrogen/phosphorus limitation, TAG production can be promoted if the supply of inorganic carbon is
623 abundant (Peng et al., 2014). TAGs can also be synthesized and accumulated when inorganic carbon is limited by invoking
624 the recycling of IPLs such as glycolipids and phospholipids (Peng et al., 2014). Thus, the higher proportions of SQs and DGs
625 in the high pH/low CO₂(aq) surface waters of our experiment could be in part related to their recycling under CO₂ limitation.

626

627 Overall, our results are consistent with other experimental data in that pH_T impacts the distribution of IPL head groups amongst
628 certain phytoplankton groups. For instance, the relatively high glycolipid abundances in surface samples with higher pH_T (most
629 notably SQ and DG, see Fig. S1) are likely not related to direct effects on membrane fluidity, but rather to the availability of
630 inorganic carbon and its effect on the recycling of phospholipids (as well as MGs), potentially for TAG synthesis. While our
631 results are consistent with the so far observed IPL substrates for TAG synthesis (Dahlqvist et al., 2000; Yoon et al., 2012),
632 additional analyses of TAG concentration and their fatty acid compositions amongst the phytoplanktonic community would
633 aid in tracing the extent of membrane lipid degradation as a source of acyl units, as well as to trace the location of these
634 biosynthetic pathways in the cell. Such work would aid in determining the extent to which TAG synthesis and IPL recycling
635 relegates phytoplankton classes to certain depths of the water column based on the combined effects of nutrient availability
636 and pH_T (amongst other variables; e.g. light, temperature, O_2 .)

637

638 4.2.3 Oxygen

639 Despite the harvesting of light energy during photosynthesis, photosynthetic organisms also rely on respiration for growth and
640 free radical scavenging under both light and dark conditions (Raven and Beardall, 2003). Specifically, the availability of O_2
641 (particularly during the dark phases or in low-light environments) influences the activation of metabolic responses, such as
642 fermentative metabolism and acetate utilization (Yang et al., 2015). Differences in dark respiration rates relative to light-
643 saturated photosynthesis among algae may confer advantages under varying oxygen availability (Geider and Osborne, 1989).
644 Thus, the ability of some organisms to perform lipid remodeling in response to oxygen stress may partially shape the
645 composition of the phytoplankton community.

646

647 In our analysis, the Random Forest models indicate a significant impact of O_2 concentration in the prediction of nearly all IPL
648 class abundances (Figs. 4-7). This pattern appears to be largely driven by differences in IPL distributions between surface
649 (oxygenated) and subsurface (hypoxic; $< \sim 1.4$ ml/L as defined by Naqvi et al., 2010) waters. Glycolipids (MG, DG, and SQ)
650 make up on average 28% more of the IPL pool in the oxygenated surface waters (~ 125 - 220 $\mu\text{mol/L O}_2$) compared to oxygen
651 deficient subsurface waters (~ 15 - 75 $\mu\text{mol/L O}_2$). The MLRs, however, show no significant relationships between individual
652 glycolipid relative abundances and O_2 concentration in surface samples (Fig. 3); this is possibly due to surface waters remaining
653 well oxygenated throughout the experiment. While several IPL moieties found in BLs, SQs, and PGs demonstrate mostly
654 negative linear relationships (Fig. 3), we suggest that the most prominent and consistent relationships are driven by a major
655 shift from oxic to hypoxic conditions (i.e., surface vs subsurface) as opposed to a sensitivity to variable O_2 concentrations.

656

657 Anaerobiosis amongst green algae has been demonstrated to impact lipid production, with significant reductions (by nearly
658 50%) in polar lipid content and concomitant increases in fatty acids (Singh and Kumar, 1992). Gombos and Murata (1991)

659 found that the cyanobacterium *Prochlorothrix hollandica* experienced a significant reduction in the relative abundance of MGs
660 that coincided with moderate increases in SQs, DGs, and PGs under low oxygen conditions. Furthermore, culture experiments
661 of anaerobically grown *Chlamydomonas reinhardtii* resulted in both decreased membrane lipid yields (most notably amongst
662 MGDGs and DGDGs; by > 50%) and an accumulation of TAGs (Hemschemeier et al., 2013). It has been noted that oxygen
663 stress appears to induce the degradation of fatty acids (~30% reduction under dark/anaerobic conditions), mostly amongst
664 unsaturated fatty acids commonly found in MGDG and DGDG membrane lipids (16:4 and 18:3) used for TAG assembly (Liu,
665 2014; Hemschemeier et al., 2013). Glycolipids (i.e., MG and DG) appear to serve as important substrates for TAG production
666 under low oxygen conditions; however, beta-oxidation of fatty acids requires oxygen to contribute to the degradation of acyl
667 groups, potentially explaining why membrane lipid degradation is attenuated under more severe hypoxia (Liu, 2014). This
668 physiological response to low oxygen conditions in subsurface waters may explain the relatively high abundance of glycolipids
669 in well oxygenated surface waters.

670

671 Dinoflagellates have been shown to exhibit particularly high dark respiration to light-saturated photosynthetic rates as
672 compared to diatoms, Chlorophyceae, or most notably cyanobacteria (Geider and Osborne, 1989), possibly pointing towards
673 a greater sensitivity to O₂ concentrations. In addition to other environmental conditions, the greater relative abundance of
674 Chlorophyceae, diatoms, and Cryptophyceae in the oxygen-deficient subsurface waters may reflect reduced respiration rates
675 amongst these algae. Differences in the proportion of glycolipids MG and DG amongst different algae, and their relative ability
676 to recycle them under oxygen stress, may play a prominent role in their individual tolerances to oxygen limitation.

677

678 Higher proportions of glycolipids in surface waters may also be due to enhanced rates of microbial degradation under oxic
679 conditions, which may be 2-4 times faster than under anoxic conditions, as tested in microcosm experiments (Ding and Sun,
680 2005). Relatively labile glycolipids can accumulate in the dissolved organic carbon pool (Gašparović et al., 2013). This
681 observation aligns with the slower breakdown of SQs compared to phospholipids observed in IPL degradation experiments
682 under aerobic conditions (Brandsma, 2011). This accumulation process, however, is unlikely in regions of the water column
683 with large numbers of active living cells, and highly active bacterial degradation. In fact, the distributions of IPLs across the
684 ODZ of the ETSP indicate minor contributions of exported IPLs to greater depths, suggesting high surface recycling (Cantarero
685 et al., 2020). However, specific experimental observations encompassing oxygen gradients ranging from well-oxygenated to
686 fully anoxic conditions are necessary to derive more robust conclusions.

687

688 4.2.4 Temperature

689 Phytoplankton have been shown to respond variably to high growth temperatures depending on their individual tolerances
690 (Huertas et al., 2011). Photosynthesis is considered the most heat-sensitive cellular function in photoautotrophs (Berry and
691 Björkman, 1980). In this section we discuss the potential lipidomic responses to heat stress within the IPL distributions of the

692 phytoplanktonic community. Temperature fluctuations affect membrane fluidity, a phenomenon commonly controlled by fatty
693 acid desaturases (Sakamoto and Murata 2002) that catalyze the production of unsaturated/saturated fatty acids to
694 increase/decrease membrane fluidity, respectively (Lyon and Mock 2014). We did not see evidence for temperature effects on
695 the degree of unsaturation in our data (see Fig. S2). This is likely due to the overall narrow temperature range observed during
696 the experiment (17.3 - 21.6 °C), which mirrors the natural variability observed in Callao (average monthly ranges ~16.6-19.6
697 °C from 2017 to 2019 (Masuda et al., 2023).

698

699 Despite the restricted temperature range and its lack of impact on the unsaturation degree of core lipids, the random forest
700 analyses identified temperature as a significant variable in predicting all IPL classes based on their polar head groups aside
701 from DG and PE (Figs. 4-7). This suggests that the response to temperature may vary among different IPLs classes. The MLRs
702 indicate consistently positive relationships between several glycolipids and temperature, suggesting a potential physiological
703 compensation via membrane compositions for higher temperatures. Gašparović et al. (2013) noted an accumulation of
704 glycolipids at temperatures >19 °C in the northern Adriatic Sea, particularly from cyanobacterial synthesis of MGs. The
705 sensitivity of photoautotrophs to thermal stress was also explored by Yang et al. (2006), who showed that DGs and MGs both
706 increase the thermal stability of photosystem II, while phospholipids significantly decrease it. Experiments with a wild-type
707 and mutant *Chlamydomonas reinhardtii* have shown that SQs are an essential component of thylakoid membranes to maintain
708 stability under heat stress (Sato et al., 2003), although at considerably more extreme temperatures (41 °C). Heat stress has also
709 been linked to the production of TAGs (Elsayed et al., 2017; Fakhry and El Maghraby, 2015), which can draw acyl units from
710 degraded membrane lipids (Holm et al., 2022).

711

712 Interestingly, the relative abundance of DGs in our experiment shows the most prominent (R^2 of 0.35-0.44), and statistically
713 significant ($p < 0.05$), linear relationship with temperature (see Fig. S3A). While temperature was not identified as an important
714 variable to the prediction of DGs in either decision tree analysis, this may be due to other covariates, such as pH and O_2 ,
715 masking the effect of temperature. Our results indicate that phytoplankton may either produce DGs in greater abundance to
716 alleviate thermal instability in photosystem II, or preferentially degrade other thylakoid membranes (i.e., PGs, SQs, or MGs)
717 in response to heat stress, leaving the remaining IPL pool relatively enriched in DGs. While several individual MG and SQ
718 molecules did demonstrate linear responses to temperature (Fig. 3), other stressors such as N availability, pH, and light levels
719 may confound the effects of temperature in the overall abundance of these lipid classes.

720 **4.2.5 Light Availability**

721 Bach et al. (2020) considered the overall productivity in these mesocosm experiments to be co-limited by N and light
722 availability, which have been identified as key limiting factors in eastern boundary upwelling systems (Messié and Chavez,
723 2015). In our experiment, initial high biomass productivity led to self-shading effects that significantly reduced the PAR (Bach
724 et al., 2020). While the maximum photon flux densities measured at noon over the course of the experiment were ~500 – 600

725 $\mu\text{mol m}^{-2}\text{s}^{-1}$, only ~5-22% and < 4% were measured in surface (~2 m) and subsurface (17 m) waters, respectively, from all four
726 mesocosms. While both depth-integrated samples in our experiment are likely from light-limited planktonic communities,
727 most PAR values (> 15% i.e., 75-132 $\mu\text{mol m}^{-2}\text{s}^{-1}$) in surface waters still demonstrate sufficiently high levels that can affect
728 lipid production and accumulation (Gonçalves et al., 2013) especially under the combined effects of N-deprivation (Yeesang
729 and Cheirsilp, 2011; Jiang et al., 2011).

730
731 Light levels are identified by the Random Forest analyses to be a significant variable in the prediction of MGs, SQs, PGs, and
732 PCs (Figs. 4, 6, and 7). While few studies have explored the direct effects of irradiance levels on IPL headgroup distributions,
733 experimental cultures of *Tichocarpus crinitus* found increased IPL production of SQs, PGs, and PCs amongst shade-grown
734 algae (Khotimchenko and Yakovleva, 2005). In *Tichocarpus crinitus* cultures, MGs, one of the most abundant thylakoid lipids,
735 show decreased abundances under low light conditions (Khotimchenko and Yakovleva, 2005). Our results show that both MGs
736 and SQs are present in greater relative and absolute abundances in the surface waters where light is less limited or potentially
737 inhibitive at times, suggesting an impact on thylakoid lipid compositions to maintain efficient photosynthetic rates under
738 changing light conditions. MGs have been shown to provide important photoprotective and antioxidant mechanisms in diatoms
739 (Wilhelm et al., 2014), potentially explaining their higher abundance in the surface waters and the significance of light in the
740 Random Forest models. While the exact function of SQs in thylakoid membranes remains unclear, they have been observed
741 to act as an antagonist to the aggregating action of MGs (Goss et al., 2009), leading to a disaggregating effect on light harvesting
742 complexes (Wilhelm et al., 2014). The latter potentially reflects planktonic responses to variable PAR (5-22%) in the surface
743 via adjustment of the proportions of SQs and MGs in the thylakoids (Gabruk et al., 2017; Nakajima et al., 2018).

744
745 The PC lipid class, primarily found in extrachloroplast membranes (Mimouni et al., 2018), consistently exhibits greater relative
746 abundance in the subsurface compared to surface waters. We suggest that light levels at depth may play a role (albeit a
747 secondary one, see Fig. S3B) in non-chloroplast IPL production when algal cells are configured for rapid growth/reproduction.
748 Conversely, under higher light as well as under the combined effects of DIC and N limitation at the surface, algal cells are
749 more prone to survival responses such as TAG production at the expense of IPLs. PG can be found in extrachloroplast
750 membranes but is also an essential component of photosystems I and II, with important roles in electron transport processes
751 (Sakurai et al., 2003; Wada and Murata, 2009; Kobayashi et al., 2017). The overall abundance of PGs contributing to the total
752 IPL pool may be influenced by varying production of certain non-chloroplast membranes under lower light conditions, and
753 other thylakoid membranes under high light conditions, thus possibly explaining the highly variable overall contribution of
754 PGs to the IPL pool. Additional analyses of specific fatty acid structures from intact PGs may illuminate sources within the
755 cell, i.e., thylakoid PGs and extrachloroplastic PGs.

756
757 Light intensity has also been shown to have contradictory impacts on fatty acid composition, with some analyses observing
758 increased unsaturation under high light intensity (Liu et al., 2012; Pal et al., 2011). Others observed that excess light energy

759 induces synthesis of saturated (SFAs) or monounsaturated (MUFAs) fatty acids in several algal species to prevent
760 photochemical damage, or the synthesis of polyunsaturated fatty acids (PUFA) for the maintenance of photosynthetic
761 membranes under low light conditions (Khoeyi et al., 2012, Fabregas et al., 2004, Sukenik et al., 1993; Orcutt and Patterson,
762 1974). However, we see limited evidence in this experiment of a direct correlation between light intensities and fatty acid
763 composition in the multiple linear regressions (Fig. 3). This may be related to differences in optimal irradiance levels between
764 algal groups overlapping to confound any clear patterns.

765

766 Given that the normalized PAR in surface waters remains <25%, and that light appears as a variable of significant but secondary
767 importance in the random forest models, our results suggest that under these experimental conditions, low or variable light
768 availability may amplify the effects of other environmental stressors (i.e., nitrogen availability, oxygen concentration,
769 temperature, and inorganic carbon availability). The effects of self-shading from high biomass production early in the
770 experiment, when greater nutrient availability was high, likely contributed to the markedly different IPL distributions observed
771 between surface and subsurface waters. As a result, the fluctuations in PAR may play a role in the observed variations in the
772 relative proportions of prevalent thylakoid membrane IPLs, including MGs, SQs, and PGs.

773

774 **4.3 Implications of IPL Remodeling in Phytoplankton Membranes**

775 We expect the ongoing changing conditions in the ETSP, such as rising temperatures, ocean acidification, expanding ODZs,
776 and shifts in upwelling-driven nutrient supply, to instigate multiple physiological responses amongst phytoplankton
777 communities. IPL remodeling and the reallocation of resources among algae are likely to have cascading effects on the
778 composition of phytoplanktonic communities, the nutritional value of algal biomass to higher trophic levels, and the cycling
779 of organic carbon and nitrogen in the upper ocean. Here, we explore the potential consequences of these physiological
780 responses to environmental conditions and outline future areas of investigation to better constrain the impacts of IPL
781 remodeling on marine biogeochemistry.

782

783 **4.3.1 Relative adaptability of Phytoplankton Classes to environmental change**

784 IPL classes are either partitioned to the thylakoid membranes (i.e., MG, DG, SQ, and PG) in variable distributions to maintain
785 photosynthetic function, or to extraplastidic membranes under growth/reproductive phases (BL, PC, PE, and PG). As
786 environmental conditions change, the ability of phytoplankton to adjust these IPL compositions may be an important driver
787 controlling the phytoplankton community structure. Within a few days of the ODZ water addition, the mesocosms became
788 oligotrophic, which coincided with a major shift in phytoplankton groups, from predominantly diatoms, Chlorophyceae, and
789 Cryptophyceae to a dominance of ‘survivalist’ mixotrophic dinoflagellates. An obvious advantage of mixotrophic

790 dinoflagellates to the largely N-limited conditions of this experiment is their ability to extract N from the DON pool, and a
791 lower dependence on light compared to the other previously mentioned phytoplankton groups.

792
793 To contextualize the impacts of IPL remodeling on the phytoplanktonic community, we performed an additional random forest
794 analysis to identify the most important IPLs (both individual moieties and polar head group totals) in the prediction of
795 individual phytoplankton classes. We applied this analysis to identify what IPL remodeling processes may be more readily
796 available to each major phytoplankton class in this experiment (Fig. 8). While all the phytoplankton classes are likely to
797 produce each IPL class to varying extents, the differences in their relative distributions may provide insight into differences in
798 phytoplankton adaptability under changing environmental conditions. Dinoflagellates are heavily associated with high
799 abundances of the glycolipids SQ and DG, with far less apparent dependence on phospholipids and MGs (Fig. 8). The
800 dominance of dinoflagellate biomass is attributed to the severe scarcity of inorganic nitrogen and relatively low light intensity
801 due to self-shading effects (Bach et al., 2020). Dinoflagellates may also take advantage of the recycling of N-bearing PCs and
802 BLs to alleviate nitrogen limitation or to produce energy storing TAGs. The high proportion of DGs and SQs and recycling of
803 MGs may also prove advantageous under high pH/low pCO₂ conditions in surface waters, alleviating pH stressors, or the
804 energy investment in active HCO₃⁻ transport for photosynthesis. These IPL remodeling strategies may have played a role in
805 the dominance of dinoflagellates under the post-upwelling experimental conditions.

806
807 In the early phases of the experiment and when inorganic N is readily available, diatoms (and to a lesser extent Cryptophyceae
808 and Chlorophyceae) dominate the water column biomass. Each of these phytoplankton classes (as well as *Synechococcus*)
809 indicates a greater dependence of the N-bearing PCs and/or BLs, potentially signaling a reduced capacity to scavenge these
810 extrachloroplastic IPLs within the cell for N, or as substrates for TAG production. Notably, these phytoplankton consistently
811 make up a greater proportion of the total chl-a pool in subsurface waters, suggesting an ability to accommodate the lower O₂
812 concentrations and pH in exchange for greater N availability (see summary in Fig. 8). Some of this adaptability may be related
813 to the recycling of MGs for additional acyl units under hypoxia (most likely amongst Chlorophyceae and *Synechococcus*),
814 and/or the generally higher relative production of structural membrane lipids under low light growth conditions (see impact of
815 light discussion above).

816
817 In the Eastern Tropical South Pacific (ETSP), upwelling events exhibit a distinctive trend of increasing frequency and intensity,
818 setting it apart from other eastern boundary systems (Abrahams et al., 2021; Oyarzún and Brierley, 2019). This phenomenon
819 brings about important changes in environmental conditions, including a decrease in sea surface temperature (~0.37°C, average
820 from 1982 to 2019, Abrahams et al., 2021) alongside oxygen reduction and reduced pH in the coastal zones of the region
821 (Pitcher et al., 2021). Simultaneously, there is an observed boost in primary productivity (Gutierrez et al., 2011; Tretkoff,
822 2011). The impact of strong upwelling, followed by rapid thermal stratification when upwelling subsides, could signify abrupt
823 changes that affect the community structure of phytoplankton (Gutierrez et al., 2011). Such environmental changes favor

824 species better adapted to stress conditions, such as mixotrophic dinoflagellates and silicoflagellates, at the expense of diatom
825 populations (Hallegraeff, 2010), which could translate to a decrease in highly nutritious saturated fatty acids for higher trophic
826 levels (Hausse et al., 2012). Furthermore, a potential reduction in diatom biomass and diversity could have consequences on
827 the ocean biological carbon pump (Tréguer et al., 2018).

828

829 Under the ongoing and projected scenarios of climate change, our mesocosm experiment demonstrates how shifts in the
830 phytoplankton community translate into changes in the lipid composition of their cell membranes. This adds weight to the
831 school of thought that lipid remodeling amongst the phytoplankton community could have repercussions at higher trophic
832 levels, as recently discussed by Holm et al. (2022), and on ocean biogeochemistry as we discuss below.

833

834 **4.3.2 Cycling of Carbon, Nitrogen, and Sulfur**

835 Combined, neutral (TAGs) and polar lipids (IPLs) make up on the order of 17.6% to 34.7% of the cell by dry weight under N-
836 replete and N-deprived conditions, respectively (Morales et al., 2021), with other environmental stressors able to compound
837 the accumulation of neutral lipids (Zienkiewicz et al., 2016). This represents a considerable portion of algal cellular carbon,
838 and total water column carbon stocks that supply the transfer of fatty acids to higher trophic levels (Twining et al., 2020).
839 Trophic transfer of fatty acids to grazing zooplankton may be affected by the relative contribution of polar and neutral lipids,
840 as they can have significantly different turnover rates (Burian et al., 2020). This suggests that the relative concentrations of
841 TAGs/IPLs in phytoplanktonic communities may impact the rates of fatty acid remineralization or uptake into higher trophic
842 levels. Additionally, while our analysis did not focus on individual fatty acid structures, other experiments investigating the
843 effects of increasing pCO₂ and nitrogen deficiency have demonstrated a reduction in the relative production of essential fatty
844 acids resulting in negative reproductive effects on primary consumers (Meyers et al., 2019). In this context, our IPL results
845 reveal modifications (among polar head groups, carbon numbers, and unsaturations) in response to divergent environmental
846 conditions. However, further investigation of the relative concentrations and turnover rates between TAGs and IPLs, in
847 addition to the production of essential fatty acids, are critical next steps in assessing the impacts of IPL remodeling on trophic
848 transfer processes.

849

850 While IPLs are not a major source of cellular N compared to proteins, the highly labile nature of these molecules after cell
851 death may be a potential source of rapidly recycled N via bacterial hydrolysis. On average, N-bearing IPLs such as PCs or
852 BLs, consist of ~2% N by molecular weight (estimated based on a typical 700g/mol betaine lipid). Based on their abundance,
853 they could contribute as much as 10.7 nmol/L of inorganic N in the highly N depleted surface waters of this experiment.
854 Inorganic N species are exceedingly low, and often below the limit of detection (< ~0.1 μmol/L, see methods for details),
855 particularly in the surface samples for most of the experiment after the OMZ water addition. Thus, it is possible that the rapid
856 degradation and recycling of N from IPLs could prove to be an additional supply of N under extremely limiting conditions.

857 Given the diel variability in TAG production via eukaryotic phytoplankton and the potential impacts on energy and carbon
858 fluxes (Becker et al., 2018), further analysis is needed to determine at what temporal scale IPLs may be recycled for TAG
859 synthesis. While Becker et al. (2018) did not find evidence of diacylglycerol transferase (DGAT) activity related to diel cycles,
860 additional investigations of other transferases or lipases relevant to the degradation of IPLs (e.g., PDAT or PGD) are critical.

861

862 IPLs may also be an important intermediate in the surface ocean sulfur cycle. Sulfur metabolites produced by phytoplankton
863 (Durham et al., 2019) play central roles in microbial food webs by functioning in metabolism, contributing to membrane
864 structure, supporting osmotic and redox balance, and acting as allelochemicals and signaling molecules (Moran and Durham,
865 2019). SQs are highly abundant IPLs, particularly in surface waters, and can constitute up to 60 nmol S/L, potentially
866 contributing to a significant proportion of the dissolved organic S in this region (ranging from ~100-225 nmol/L; Lennartz et
867 al., 2019). The ability to catabolize SQs is widespread in heterotrophic bacteria and provides a highly ubiquitous source of
868 sulfur (and carbon) substrates in the synthesis of other essential sulfur metabolites (Speciale et al., 2016). As such, SQs are
869 considered major contributors to the global biosulfur cycle (Goddard-Borger and Williams, 2017) and their considerable
870 production in phytoplankton membranes may be augmented by changes in temperature, light availability (i.e., shading effects),
871 and pH (see discussion above).

872

873 Lipids are also sources of dissolved organic carbon (DOC) following hydrolysis by bacterial extracellular enzymes (Myklestad,
874 2000). Lipids have been observed as the most highly aged component of DOC and are considerably longer lived than lipids
875 found in suspended POC (Loh et al., 2004). However, much of the DOC pool remains uncharacterized (Nebbioso and Piccolo,
876 2013; Hansell and Carlson, 2014) and little is known regarding the specific processes forming refractory DOC fractions
877 (Hansell, 2013). Yet, preliminary estimates of the total production of relatively refractory DOC (>100-year lifetime) suggest
878 potential significance to global biogeochemistry (Legendre et al., 2015). Furthermore, it is yet unclear as to how DOC cycling
879 may be affected by changing ocean conditions (Wagner et al., 2020). Understanding the degradation pathways involved with
880 abundant lipid pools and how they may contribute to the DOC pool in the surface ocean is of crucial importance to constraining
881 the fluxes of refractory organic carbon pools.

882

883 **5 Conclusions**

884 We investigated the potential for phytoplankton to evoke lipid remodeling in response to multiple environmental stressors
885 during a two-month mesocosm experiment in the Eastern Tropical South Pacific Ocean off the coast of Peru. Our study is
886 motivated by the need of understanding how the expected changes in oceanographic conditions due to climate forcing in this
887 area will impact the phytoplanktonic community driving primary productivity in the surface ocean, the chemistry of their cell
888 membranes, and thus the chemical composition of particulate organic matter. A key aspect of our efforts was to statistically

889 separate the relative roles of phytoplankton community composition and lipid remodeling in response to multiple
890 environmental stressors on the composition of the environmental algal lipidome over time. By using a combination of multiple
891 linear regressions, classification and regression trees, and random forest analyses, we report evidence of multiple
892 environmental variables potentially imparting controls on IPL head groups, many of which are known to have specific
893 functions in the chloroplast. The main takeaways of our study include:

- 894 ● IPLs are effective predictors of changes in the prevailing sources of phytoplankton biomass throughout the experiment.
- 895 ● The proportion of glycolipids (MG and SQ) increases at higher temperatures, possibly to maintain thermal stability of the
896 photosynthetic apparatus in response to thermal stress.
- 897 ● The relationship between light levels and the distribution of MGs and PGs possibly invokes photoprotective and
898 antioxidant mechanisms provided by MGs, as well as the role of PGs in electron transport processes in photosystems I
899 and II.
- 900 ● Differences in the abundance of glycolipids between surface and subsurface waters appear to covary with oxygen
901 availability. We expect this difference to be driven by the degradation of MGs and DGs under anaerobiosis or oxygen
902 stress.
- 903 ● The reduction in N-bearing IPLs (i.e. BLs and PE) and the higher abundance of non-N-bearing IPLs (i.e., PG, SQ and
904 MG) under more N-limited conditions suggests a possible IPL substitution mechanism to compensate for N limitation.
- 905 ● Whereas our study does not include the analysis of TAGs, our results are consistent with broader work suggesting that
906 IPLs may be used as a substrate for the generation of acyl chains in TAG production in response to environmental stressors
907 such as N limitation, variable pH or inorganic carbon availability, hypoxia, and varying light levels. However, such
908 mechanism in this mesocosm experiment remains to be tested in future work.
- 909 ● The cellular adaptations listed above likely contribute to the observed shifts in cellular content from structural or
910 extrachloroplastic membrane lipids (i.e., PCs, PEs, BLs, and certain PGs) under high growth conditions, to
911 thylakoid/plastid membrane lipids (i.e., MGs, DGs, SQs, and certain PGs) while exposed to environmental stressors.

912 We hypothesize that these remodeling processes may involve major shifts in the elemental stoichiometry of the cell, and thus
913 alter the fluxes of C, N, and S to higher trophic levels, signaling potential impacts on the broader cycling of these biorelevant
914 elements under different scenarios of future environmental change. Therefore, we suggest that future studies addressing the
915 biogeochemical consequences of climate change in the Eastern Tropical South Pacific Ocean must include the role of lipid
916 remodeling in phytoplankton.

917

918 **Data availability**

919

920 The environmental study data are available at: <https://doi.org/10.1594/PANGAEA.923395> (Bach et al., 2020). Biomarkers
921 metadata that generates and supports the findings of this study and R code are available in: [https://github.com/Guachan/IPLS-](https://github.com/Guachan/IPLS-KOSMOS/tree/0.1.0)
922 [KOSMOS/tree/0.1.0](https://doi.org/10.5281/zenodo.10408453) (<https://doi.org/10.5281/zenodo.10408453>, Cantarero, 2023).

923

924 **Author contribution**

925 JS and SC designed the study. JS funded the study. JS and CV funded sample collection during the mesocosm experiment. UL
926 and LTB designed, funded, organized, and carried out the mesocosm experiment. PA, JS, LTB, and UR carried out sample
927 collection. SIC led laboratory and analytical work with the assistance of ND and under the supervision of JS. SEI carried out
928 data analysis. SIC, JET, BCS, and BR performed statistical analyzes. SIC wrote the manuscript with major editorial
929 contributions from EF, HA, and JS and with comments from all co-authors.
930

931 **Competing interests**

932 The authors declare that they have no conflict of interest. At least one of the (co-)authors is a member of the editorial board of
933 Biogeosciences.
934

935 **Acknowledgments**

936 We extend our gratitude to all participants in the KOSMOS Peru 2017 study for their invaluable assistance in mesocosm
937 sampling and maintenance. Our special thanks go to the dedicated staffs from GEOMAR-Kiel and IMARPE for their support
938 throughout the planning, preparation, and execution of this study. We are particularly grateful to A. Ludwig, M. Graco, D.
939 Gutierrez, A. Paul, S. Feiersinger, K. Schulz, J.P. Bednar, P. Fritsche, P. Stange, A. Schukat, and M. Krudewig. We also
940 express our appreciation to the captains and crews of BAP Morales, IMARPE VI, and BIC Humboldt for their support during
941 the deployment and recovery of the mesocosms. We extend special thanks to the Marina de Guerra del Perú, specifically the
942 submarine section of the navy in Callao, the Dirección General de Capitanías y Guardacostas, and the Club Náutico Del Centro
943 Naval. The KOSMOS Peru 2017 took place within the framework of the cooperation agreement between IMARPE and
944 GEOMAR through the German Federal Ministry of Education and Research (BMBF) project ASLAEEL 12-016 and the national
945 project Integrated Study of the Upwelling System off Peru developed by the Directorate of Oceanography and Climate Change
946 of IMARPE, PPR 137 CONCYTEC. We acknowledge all members of the Organic Geochemistry Laboratory in addition to K.
947 Rempfert, S. Kopf, T. Marchitto, N. Lovenduski at the University of Colorado Boulder, and M. Long at NCAR, for fruitful
948 discussions.
949

950 **Financial support**

951 This study was funded by the US National Science Foundation CAREER Award 2047057 "Microbial Lipidomics in Changing
952 Oceans" (MILCO) to J. Sepúlveda. S. Cantarero and J. Sepúlveda acknowledge additional support from the Department of
953 Geological Sciences and the Center for the Study of Origins at the University of Colorado Boulder. We thank the Millennium
954 Institute of Oceanography (IMO) ICN12_019 through the Agencia Nacional de Investigación y Desarrollo (ANID)—
955 Millennium Science Initiative Program—for providing funding for sample collection. The KOSMOS Peru 2017 was funded
956 by the Collaborative Research Centre SFB 754 Climate-Biogeochemistry Interactions in the Tropical Ocean, funded by the
957 German Research Foundation (DFG) to U. Riebesell. Additional funding was provided by the EU project AQUACOSM
958 through the European Union's Horizon 2020 research and innovation program under grant agreement no. 731065 and through
959 the Leibniz Award 2012, granted to Ulf Riebesell.
960

961 **References**

962 Abida, H., Dolch, L.J., Meř, C., Villanova, V., Conte, M., Block, M.A., Finazzi, G., Bastien, O., Tirichine, L., Bowler, C.,
963 Rébeillé, F., Petroustos, D., Jouhet, J., Maréchal, E.: Membrane glycerolipid remodeling triggered by nitrogen and
964 phosphorus starvation in *Phaeodactylum tricornutum*. *Plant Physiology*, 167, 118–136, ,
965 <https://doi.org/10.1104/pp.114.252395>, 2015. Abrahams, A., Schlegel, R. W., and Smit, A. J.: Variation and change of
966

972 upwelling dynamics detected in the world's eastern boundary upwelling systems, *Front. Mar. Sci.*, 8, 626411, doi:
973 10.3389/fmars.2021.626411, 2021.

974 Arístegui, J. and Harrison, W. G.: Decoupling of primary production and community respiration in the ocean: Implications for
975 regional carbon studies, *Aquat. Microb. Ecol.*, 29(2), 199–209, doi:10.3354/ame029199, 2002.

976 Arrigo, K. R.: Marine microorganisms and global nutrient cycles, *Nature*, 437(7057), 349–355, doi:10.1038/nature04159,
977 2005.

978 Azov, Y.: Effect of pH on inorganic carbon uptake in algal cultures, *Appl. Environ. Microbiol.*, 43(6), 1300–1306,
979 doi:10.1128/aem.43.6.1300-1306.1982, 1982.

980 Bach, L. T., Alvarez-Fernandez, S., Hornick, T., Stuhr, A. and Riebesell, U.: Simulated ocean acidification reveals winners
981 and losers in coastal phytoplankton, *PLoS One*, 12(11), 1–22, doi: 10.1371/journal.pone.0188198, 2017.

982 Bach, L. T., Paul, A. J., Boxhammer, T., von der Esch, E., Graco, M., Schulz, K. G., Achterberg, E., Aguayo, P., Arístegui, J.,
983 Ayón, P., Baños, I., Bernales, A., Boegeholz, A. S., Chavez, F., Chavez, G., Chen, S. M., Doering, K., Filella, A., Fischer,
984 M., Grasse, P., Haunost, M., Hennke, J., Hernández-Hernández, N., Hopwood, M., Igarza, M., Kalter, V., Kittu, L.,
985 Kohnert, P., Ledesma, J., Lieberum, C., Lischka, S., Löscher, C., Ludwig, A., Mendoza, U., Meyer, J., Meyer, J.,
986 Minutolo, F., Cortes, J. O., Piiparinen, J., Sforza, C., Spilling, K., Sanchez, S., Spisla, C., Sswat, M., Moreira, M. Z. and
987 Riebesell, U.: Factors controlling plankton community production, export flux, and particulate matter stoichiometry in
988 the coastal upwelling system off Peru, *Biogeosciences*, 17(19), 4831–4852, doi:10.5194/bg-17-4831-2020, 2020.

989 Bakun, A., Field, D. B., Redondo-Rodriguez, A. and Weeks, S. J.: Greenhouse gas, upwelling-favorable winds, and the future
990 of coastal ocean upwelling ecosystems, *Glob. Chang. Biol.*, 16(4), 1213–1228, doi:10.1111/j.1365-2486.2009.02094.x,
991 2010.

992 Barlow, R. G., Cummings, D. G. and Gibb, S. W.: Improved resolution of mono- and divinyl chlorophylls a and b and
993 zeaxanthin and lutein in phytoplankton extracts using reverse phase C-8 HPLC, *Mar. Ecol. Prog. Ser.*, 161, 303–307,
994 <http://www.jstor.org/stable/24859034>, 1997.

995 Becker, K.W., Collins, J.R., Durham, B.P., Groussman, R.D., White, A.E., Fredricks, H.F., Ossolinski, J.E., Repeta, D.J.,
996 Carini, P., Armbrust, E.V. and Van Mooy, B.A., Daily changes in phytoplankton lipidomes reveal mechanisms of energy
997 storage in the open ocean. *Nature communications* 9, 5179, <https://doi.org/10.1038/s41467-018-07346-z>, 2018.

998 Behrenfeld, M. J., O'Malley, R. T., Siegel, D. A., McClain, C. R., Sarmiento, J. L., Feldman, G. C., Milligan, A. J., Falkowski,
999 P. G., Letelier, R. M. and Boss, E. S.: Climate-driven trends in contemporary ocean productivity, *Nature*, 444(7120),
1000 752–755, doi:10.1038/nature05317, 2006.

1001 Benjamini, Y., and Yosef Hochberg, Y., Controlling the False Discovery Rate: A Practical and Powerful Approach to Multiple
1002 Testing, *Journal of the Royal Statistical Society: Series B (Methodological)*, 57, 289–300, doi:10.1111/j.2517-
1003 6161.1995.tb02031.x, 1995.

1004 Berry, J. and Bjorkman, O.: Photosynthetic Response and Adaptation to Temperature in Higher Plants, *Annu. Rev. Plant*
1005 *Physiol.*, 31(1), 491–543, doi:10.1146/annurev.pp.31.060180.002423, 1980.

1006 Brandsma, J.: The origin and fate of intact polar lipids in the marine environment, PhD thesis, Dept. of Marine Organic
1007 Biogeochemistry, Royal Netherlands Institute for Sea Research (NIOZ), pp. 224, ISBN: 978-90-6266-286-9, 2011.

1008 Bligh, E. G., and Dyer, W.J.: A rapid method of total lipid extraction and purification, Canadian journal of biochemistry and
1009 physiology, 37(8), 911-917, doi:10.1139/o59-099, 1959.

1010 Biau G., and Scornet E. A random forest guided tour. Test; 25(2): 197–227, <https://doi.org/10.1007/s11749-016-0481-7>, 2016.

1011 Boulesteix, A. L., Janitza, S., Kruppa, J., & König, I. R.: Overview of random forest methodology and practical guidance with
1012 emphasis on computational biology and bioinformatics. Wiley Interdisciplinary Reviews: Data Mining and Knowledge
1013 Discovery, 2(6), 493–507, <https://doi.org/10.1002/widm.1072>, 2012.

1014 Breiman, L., Friedman, J.H., Olshen, R.A., & Stone, C.J.: Classification And Regression Trees (1st ed.), Chapman and
1015 Hall/CRC, <https://doi.org/10.1201/9781315139470>, 1984.

1016 Breiman, L.: Random Forests, Mach. Learn., 45, 5–32, <https://doi.org/10.1023/A:1010933404324>, 2001.

1017 Browning, T. J., Rapp, I., Schlosser, C., Gledhill, M., Achterberg, E. P., Bracher, A. and Le Moigne, F. A. C.: Influence of
1018 Iron, Cobalt, and Vitamin B12 Supply on Phytoplankton Growth in the Tropical East Pacific During the 2015 El Niño,
1019 Geophys. Res. Lett., 45(12), 6150–6159, doi:10.1029/2018GL077972, 2018.

1020 Bronk, D. A., See, J. H., Bradley, P., & Killberg, L.: DON as a source of bioavailable nitrogen for phytoplankton.
1021 Biogeosciences, 4(3), 283–296. <https://doi.org/10.5194/bg-4-283-2007>, 2007.

1022 Burian, A., Nielsen, J. M., Hansen, T., Bermudez, R. and Winder, M.: The potential of fatty acid isotopes to trace trophic
1023 transfer in aquatic food-webs, Philos. Trans. R. Soc. B Biol. Sci., 375(1804), doi:10.1098/rstb.2019.0652, 2020.

1024 Cantarero, S., Henríquez-Castillo, C., Dildar, N., Vargas, C., von Dassow, P., Cornejo-D’Ottone, M. and Sepúlveda, J.: Size-
1025 fractionated contribution of microbial biomass to suspended organic matter in the Eastern Tropical South Pacific oxygen
1026 minimum zone, Front. Mar. Sci., 7:540643. doi: 10.3389/fmars.2020.540643, 2020.

1027 Capone, D. G. and Hutchins, D. A.: Microbial biogeochemistry of coastal upwelling regimes in a changing ocean, Nat. Geosci.,
1028 6(9), 711–717, doi:10.1038/ngeo1916, 2013.

1029 Carter, B. R., Radich, J. A., Doyle, H. L. and Dickson, A. G.: An automated system for spectrophotometric seawater pH
1030 measurements, Limnol. Oceanogr. Methods, 11(JAN), 16–27, doi:10.4319/lom.2013.11.16, 2013.

1031 Chavez, F. P. and Messié, M.: A comparison of Eastern Boundary Upwelling Ecosystems, Prog. Oceanogr., 83(1–4), 80–96,
1032 doi:10.1016/j.pocean.2009.07.032, 2009.

1033 Chen, S., Riebesell, U., Schulz, K. G., Esch, E. Von Der, Achterberg, E. P. and Bach, L. T.: Temporal dynamics of surface
1034 ocean carbonate chemistry in response to natural and simulated upwelling events during the 2017 coastal El Niño near
1035 Callao, Peru., Biogeosciences, 19,295-312, <https://doi.org/10.5194/bg-19-295-2022>, 2022.

1036 Chen, X., and H. Ishwaran.: Random forests for genomic data analysis. Genomics 99: 323–329,
1037 <https://doi.org/10.1016/j.ygeno.2012.04.003>, 2012.Coverly, S., Kérouel, R. and Aminot, A.: A re-examination of matrix
1038 effects in the segmented-flow analysis of nutrients in sea and estuarine water, Anal. Chim. Acta, 712, 94–100,
1039 doi:10.1016/j.aca.2011.11.008, 2012.

1040 Dahlqvist, A., Ståhl, U., Lenman, M., Banas, A., Lee, M., Sandager, L., Ronne, H. and Stymne, S.: Phospholipid:diacylglycerol
1041 acyltransferase: An enzyme that catalyzes the acyl-CoA-independent formation of triacylglycerol in yeast and plants,
1042 Proc. Natl. Acad. Sci. U. S. A., 97(12), 6487–6492, doi:10.1073/pnas.120067297, 2000.

1043 Ding, H. and Sun, M. Y.: Biochemical degradation of algal fatty acids in oxic and anoxic sediment-seawater interface systems:
1044 Effects of structural association and relative roles of aerobic and anaerobic bacteria, Mar. Chem., 93(1), 1–19,
1045 doi:10.1016/j.marchem.2004.04.004, 2005.

1046 DiTullio, G. R., Geesey, M. E., Mancher, J. M., Alm, M. B., Riseman, S. F. and Bruland, K. W.: Influence of iron on algal
1047 community composition and physiological status in the Peru upwelling system, Limnol. Oceanogr., 50(6), 1887–1907,
1048 doi:10.4319/lo.2005.50.6.1887, 2005.

1049 Durham, B. P., Boysen, A. K., Carlson, L. T., Groussman, R. D., Heal, K. R., Cain, K. R., Morales, R. L., Coesel, S. N.,
1050 Morris, R. M., Ingalls, A. E. and Armbrust, E. V.: Sulfonate-based networks between eukaryotic phytoplankton and
1051 heterotrophic bacteria in the surface ocean, Nat. Microbiol., 4(10), 1706–1715, doi:10.1038/s41564-019-0507-5, 2019.

1052 Dutkiewicz, S., Ward, B. A., Monteiro, F. and Follows, M. J.: Interconnection of nitrogen fixers and iron in the Pacific Ocean:
1053 Theory and numerical simulations, Global Biogeochem. Cycles, 26(1), 1–16, doi:10.1029/2011GB004039, 2012.

1054 Dutkiewicz, S., Morris, J. J., Follows, M. J., Scott, J., Levitan, O., Dyhrman, S. T. and Berman-Frank, I.: Impact of ocean
1055 acidification on the structure of future phytoplankton communities, Nat. Clim. Chang., 5(11), 1002–1006,
1056 doi:10.1038/nclimate2722, 2015.

1057 Elsayed, K. N. M., Kolesnikova, T. A., Noke, A. and Klöck, G.: Imaging the accumulated intracellular microalgal lipids as a
1058 response to temperature stress, 3 Biotech, 7(1), doi:10.1007/s13205-017-0677-x, 2017.

1059 Missing: Fabregas et al 2004 from 4.2.5 light availability

1060 Fakhry, E. M. and El Maghraby, D. M.: Lipid accumulation in response to nitrogen limitation and variation of temperature in
1061 nannochloropsis salina, Bot. Stud., 56, 6, doi:10.1186/s40529-015-0085-7, 2015.

1062 Fan, J., Andre, C. and Xu, C.: A chloroplast pathway for the de novo biosynthesis of triacylglycerol in *Chlamydomonas*
1063 *reinhardtii*, FEBS Lett., 585(12), 1985–1991, doi:10.1016/j.febslet.2011.05.018, 2011.

1064 Fuenzalida, R., Schneider, W., Garcés-Vargas, J., Bravo, L. and Lange, C.: Vertical and horizontal extension of the oxygen
1065 minimum zone in the eastern South Pacific Ocean, Deep. Res. Part II Top. Stud. Oceanogr., 56(16), 992–1003,
1066 doi:10.1016/j.dsr2.2008.11.001, 2009.

1067 Gabruk, M., Mysliwa-Kurdziel, B., and Kruk, J.. MGDG, PG and SQDG regulate the activity of light-dependent
1068 protochlorophyllide oxidoreductase. Biochem. J. 474, 1307–1320. doi: 10.1042/BCJ20170047, 2017.

1069 Gardner, R. D., Cooksey, K. E., Mus, F., Macur, R., Moll, K., Eustance, E., Carlson, R. P., Gerlach, R., Fields, M. W. and
1070 Peyton, B. M.: Use of sodium bicarbonate to stimulate triacylglycerol accumulation in the chlorophyte *Scenedesmus* sp.
1071 and the diatom *Phaeodactylum tricorutum*, J. Appl. Phycol., 24(5), 1311–1320, doi:10.1007/s10811-011-9782-0, 2012.

- 1072 Gardner, R., Peters, P., Peyton, B. and Cooksey, K. E.: Medium pH and nitrate concentration effects on accumulation of
1073 triacylglycerol in two members of the chlorophyta, *J. Appl. Phycol.*, 23(6), 1005–1016, doi:10.1007/s10811-010-9633-
1074 4, 2011.
- 1075 Gašparović, B., Godrijan, J., Frka, S., Tomažić, I., Penezić, A., Marić, D., Djakovac, T., Ivančić, I., Paliaga, P., Lyons, D.,
1076 Precali, R. and Tepić, N.: Adaptation of marine plankton to environmental stress by glycolipid accumulation, *Mar.*
1077 *Environ. Res.*, 92, 120–132, doi:10.1016/j.marenvres.2013.09.009, 2013.
- 1078 Geider, J. R. and Osborne, B. A.: Respiration and microalgal growth: a review of the quantitative relationship between dark
1079 respiration and growth, *New Phytol.*, 112(3), 327–341, doi:10.1111/j.1469-8137.1989.tb00321.x, 1989.
- 1080 Gilly, W. F., Beman, J. M., Litvin, S. Y. and Robison, B. H.: Oceanographic and Biological Effects of Shoaling of the Oxygen
1081 Minimum Zone, *Ann. Rev. Mar. Sci.*, 5(1), 393–420, doi:10.1146/annurev-marine-120710-100849, 2013.
- 1082 Goddard-Borger, and E.D., Williams, S.J., Sulfoquinovose in the biosphere: occurrence, metabolism and functions. *Biochem*
1083 *J* 1, 474 (5), 827–849, doi: <https://doi.org/10.1042/BCJ20160508>, 2017.
- 1084 Gombos, Z. and Murata, N.: Lipids and fatty acids of prochlorothrix hollandica, *Plant Cell Physiol.*, 32(1), 73–77,
1085 doi:10.1093/oxfordjournals.pcp.a078054, 1991.
- 1086
- 1087 Gonçalves, A. L., Pires, J. C., & Simões, M.: Lipid production of *Chlorella vulgaris* and *Pseudokirchneriella subcapitata*. *Int.*
1088 *J. Energy Environ. Eng.*, 4, 14, <https://doi.org/10.1186/2251-6832-4-14> 2013.
- 1089 Goss, R., Nerlich, J., Lepetit, B., Schaller, S., Vieler, A. and Wilhelm, C.: The lipid dependence of diadinoxanthin de-
1090 epoxidation presents new evidence for a macrodomain organization of the diatom thylakoid membrane, *J. Plant Physiol.*,
1091 166(17), 1839–1854, doi:10.1016/j.jplph.2009.05.017, 2009.
- 1092 Gu, X., Cao, L., Wu, X., Li, Y., Hu, Q. and Han, D.: A lipid bodies-associated galactosyl hydrolase is involved in
1093 triacylglycerol biosynthesis and galactolipid turnover in the unicellular green alga *chlamydomonas reinhardtii*, *Plants*,
1094 10(4), doi:10.3390/plants10040675, 2021.
- 1095 Guckert, J. B., and Cooksey, K.E.: Triglyceride accumulation and fatty acid profile changes in *Chlorella* (Chlorophyta) during
1096 high Ph-induced cell cycle Inhibition, *Journal of Phycology*, 26, 72-79, <https://doi.org/10.1111/j.0022-3646.1990.00072.x>, 1990.
- 1097
- 1098 Guschina, I. A., and Harwood, J. L. Algal lipids and their metabolism. In: Borowitzka, M., Moheimani, N. (eds) *Algae for*
1099 *Biofuels and Energy*. Springer, Dordrecht, pp. 17-36. https://doi.org/10.1007/978-94-007-5479-2_2, 2013.
- 1100 Gutiérrez, D., Bouloubassi, I., Sifeddine, A., Purca, S., Goubanova, K., Graco, M., Field, D., Méjanelle, L., Velazco, F., Lorre,
1101 A., Salvattecí, R., Quispe, D., Vargas, G., Dewitte, B. and Ortlieb, L.: Coastal cooling and increased productivity in the
1102 main upwelling zone off Peru since the mid-twentieth century, *Geophys. Res. Lett.*, 38(7), 1–6,
1103 doi:10.1029/2010GL046324, 2011.
- 1104 Hallegraeff, G.M. Ocean climate change, phytoplankton community responses, and harmful algal blooms: a formidable
1105 predictive challenge. *J. Phycol.* 46 (2), 220–235, <https://doi.org/10.1111/j.1529-8817.2010.00815.x>, 2010.

1106 Hansell, D. A.: Recalcitrant dissolved organic carbon fractions, *Ann. Rev. Mar. Sci.*, 5, 421–445, doi:10.1146/annurev-marine-
1107 120710-100757, 2013.

1108 Hansell, D. A., and Carlson, C.A., eds. *Biogeochemistry of marine dissolved organic matter*. Academic Press,
1109 <https://doi.org/10.1016/C2012-0-02714-7>, 2014.

1110 Harwood, J. L. and Jones, A. L.: *Lipid Metabolism in Algae.*, *Advances in Botanical Research*, 16, 1-53,
1111 [https://doi.org/10.1016/S0065-2296\(08\)60238-4](https://doi.org/10.1016/S0065-2296(08)60238-4), 1989.

1112 Hastie, T., Tibshirani, R. and Friedman, J.: *Springer Series in Statistics, Elem. Stat. Learn.*, 27(2), 83–85, doi:10.1007/b94608,
1113 2009.

1114 Hauss, H., Franz, J., and Sommer, U.: Changes in N:P stoichiometry influence taxonomic composition and nutritional quality
1115 of phytoplankton in the Peruvian upwelling, *J. Sea Res.*, 73, 74–85, <https://doi.org/10.1016/j.seares.2012.06.010>, 2012.

1116 Hemschemeier, A., Casero, D., Liu, B., Benning, C., Pellegrini, M., Happe, T. and Merchant, S. S.: COPPER RESPONSE
1117 REGULATOR1-dependent and -independent responses of the *Chlamydomonas reinhardtii* transcriptome to dark anoxia,
1118 *Plant Cell*, 25(9), 3186–3211, doi:10.1105/tpc.113.115741, 2013.

1119 Henson, S. A., Cael, B. B., Allen, S. R. and Dutkiewicz, S.: Future phytoplankton diversity in a changing climate, *Nat.*
1120 *Commun.*, 12(1), 1–8, doi:10.1038/s41467-021-25699-w, 2021.

1121 Holm, H. C., Fredricks, H. F., Bent, S. M., Lowenstein, D. P., Ossolinski, J. E., Becker, K. W., Johnson, W. M., Schrage, K.,
1122 & Van Mooy, B. A. S. Global Ocean lipidomes show a universal relationship between temperature and lipid unsaturation.
1123 *Science*, 376, 1487– 1491. <https://doi.org/10.1126/science.abn7455>, 2022.

1124 Hu, Q., Sommerfeld, M., Jarvis, E., Ghirardi, M., Posewitz, M., Seibert, M. and Darzins, A.: Microalgal triacylglycerols as
1125 feedstocks for biofuel production: Perspectives and advances, *Plant J.*, 54(4), 621–639, doi:10.1111/j.1365-
1126 313X.2008.03492.x, 2008.

1127 Huertas E., I., Rouco, M., López-Rodas, V. and Costas, E.: Warming will affect phytoplankton differently: Evidence through
1128 a mechanistic approach, *Proc. R. Soc. B Biol. Sci.*, 278(1724), 3534–3543, doi:10.1098/rspb.2011.0160, 2011.

1129 Hutchins, D. A., Hare, C. E., Weaver, R. S., Zhang, Y., Firme, G. F., DiTullio, G. R., Alm, M. B., Riseman, S. F., Maucher,
1130 J. M., Geesey, M. E., Trick, C. G., Smith, G. J., Rue, E. L., Conn, J. and Bruland, K. W.: Phytoplankton iron limitation
1131 in the Humboldt Current and Peru Upwelling, *Limnol. Oceanogr.*, 47(4), 997–1011, doi:10.4319/lo.2002.47.4.0997,
1132 2002.

1133 Hutchins, D. A. and Fu, F.: Microorganisms and ocean global change, *Nat. Microbiol.*, 2(May),
1134 doi:10.1038/nmicrobiol.2017.58, 2017.

1135 Irwin, A. J., Finkel, Z. V., Müller-Karger, F. E. and Ghinaglia, L. T.: Phytoplankton adapt to changing ocean environments,
1136 *Proc. Natl. Acad. Sci. U. S. A.*, 112(18), 5762–5766, doi:10.1073/pnas.1414752112, 2015.

1137 Jiang, L., Luo, S., Fan, X., Yang, Z. and Guo, R.: Biomass and lipid production of marine microalgae using municipal
1138 wastewater and high concentration of CO₂, *Appl. Energy*, 88(10), 3336–3341, doi:10.1016/j.apenergy.2011.03.043,
1139 2011.

- 1140 Jiang, L. Q., Carter, B. R., Feely, R. A., Lauvset, S. K. and Olsen, A.: Surface ocean pH and buffer capacity: past, present and
1141 future, *Sci. Rep.*, 9(1), 1–11, doi:10.1038/s41598-019-55039-4, 2019.
- 1142 Jin, P., Liang, Z., Lu, H., Pan, J., Li, P., Huang, Q., Guo Y., Zhong, J., Li, F., Wan, J., Overmans, S., and Xia, J.: Lipid
1143 remodeling reveals the adaptations of a marine diatom to ocean acidification. *Frontiers in Microbiology*, 12, 748445,
1144 doi: 10.3389/fmicb.2021.748445, 2021.
- 1145 Jónasdóttir, S. H.: Fatty acid profiles and production in marine phytoplankton, *Mar. Drugs*, 17(3), doi:10.3390/md17030151,
1146 2019.
- 1147 Kato, C., Masui, N., and Horikoshi, K.: Properties of obligately barophilic bacteria isolated from a sample of deep-sea sediment
1148 from the Izu-Bonin trench, *J. Mar. Biotechnol.*, 4, 96-99, <https://cir.nii.ac.jp/crid/1573105973909199488>, 1996.
- 1149 Keeling, R. F., Körtzinger, A. and Gruber, N.: Ocean deoxygenation in a warming world, *Ann. Rev. Mar. Sci.*, 2(1), 199–229,
1150 doi:10.1146/annurev.marine.010908.163855, 2010.
- 1151 Kérouel, R. and Aminot, A.: Fluorometric determination of ammonia in sea and estuarine waters by direct segmented flow
1152 analysis, *Mar. Chem.*, 57(3–4), 265–275, doi:10.1016/S0304-4203(97)00040-6, 1997.
- 1153 Khoeyi, Z. A., Seyfabadi, J. and Ramezanpour, Z.: Effect of light intensity and photoperiod on biomass and fatty acid
1154 composition of the microalgae, *Chlorella vulgaris*, *Aquac. Int.*, 20(1), 41–49, doi:10.1007/s10499-011-9440-1, 2012.
- 1155 Khotimchenko, S. V. and Yakovleva, I. M.: Lipid composition of the red alga *Tichocarpus crinitus* exposed to different levels
1156 of photon irradiance, *Phytochemistry*, 66(1), 73–79, doi:10.1016/j.phytochem.2004.10.024, 2005.
- 1157 Khotimchenko, S. V. and Yakovleva, I. M.: Effect of solar irradiance on lipids of the green alga *Ulva fenestrata* Postels et
1158 Ruprecht, *Bot. Mar.*, 47(5), 395–401, doi:10.1515/BOT.2004.050, 2004.
- 1159 Kobayashi, K., Endo, K. and Wada, H.: Specific distribution of phosphatidylglycerol to photosystem complexes in the
1160 thylakoid membrane, *Front. Plant Sci.*, 8(November), 1–7, doi:10.3389/fpls.2017.01991, 2017.
- 1161 Kong, F., Romero, I. T., Warakanont, J. and Li-Beisson, Y.: Lipid catabolism in microalgae, *New Phytol.*, 218(4), 1340–1348,
1162 doi:10.1111/nph.15047, 2018.
- 1163 Kudela, R. M., Seeyave, S., and Cochlan, W. P.: The role of nutrients in regulation and promotion of harmful algal blooms in
1164 upwelling systems, *Prog. Oceanogr.*, 85, 122–135, <https://doi.org/10.1016/j.pocean.2010.02.008>, 2010.
- 1165 Kumari, P., Bijo, A. J., Mantri, V. A., Reddy, C. R. K. and Jha, B.: Fatty acid profiling of tropical marine macroalgae: An
1166 analysis from chemotaxonomic and nutritional perspectives, *Phytochemistry*, 86, 44–56,
1167 doi:10.1016/j.phytochem.2012.10.015, 2013.
- 1168 Lam, P., Kuypers, M. M. M., Lavik, G., Jensen, M. M., Vossenberg, J. Van De, Schmid, M., Woebken, D., Amann, R., Jetten,
1169 M. S. M. and Kuypers, M. M. M.: Revising the nitrogen cycle in the Peruvian oxygen minimum zone Phyllis, *Proc. Natl.*
1170 *Acad. Sci.*, 106(12), 2192–2205, doi:10.1038/nature0415, 2009.
- 1171 Legendre, L., Rivkin, R. B., Weinbauer, M. G., Guidi, L. and Uitz, J.: The microbial carbon pump concept: Potential
1172 biogeochemical significance in the globally changing ocean, *Prog. Oceanogr.*, 134, 432–450,
1173 doi:10.1016/j.pocean.2015.01.008, 2015.

- 1174 Lennartz, S., von Hobe, M., Booge, D., Bittig, H., Fischer, T., Gonçalves-Araujo, R., Ksionzek, K., Koch, B., Bracher, A.,
1175 Röttgers, R., Quack, B. and Marandino, C.: The influence of dissolved organic matter on the marine production of
1176 carbonyl sulfide (OCS) and carbon disulfide (CS₂) in the Eastern Tropical South Pacific, *Ocean Sci. Discuss.*, (March),
1177 1–32, doi:10.5194/os-2019-1, 2019.
- 1178 Li, X., Benning, C., & Kuo, M. H.: Rapid triacylglycerol turnover in *Chlamydomonas reinhardtii* requires a lipase with broad
1179 substrate specificity. *Eukaryotic Cell*, 11(12), 1451-1462, doi: 10.1128/EC.00268-12, 2012.
- 1180 Li-Beisson, Y., Thelen, J. J., Fedosejevs, E. and Harwood, J. L.: The lipid biochemistry of eukaryotic algae, *Prog. Lipid Res.*,
1181 74, 31–68, doi:10.1016/j.plipres2019.01.003, 2019.
- 1182 Lipp, J. S., Morono, Y., Inagaki, F., and Hinrichs, K.-U.: Significant contribution of Archaea to extant biomass in marine
1183 subsurface sediments, *Nature*, 454, 991–994, <https://doi.org/10.1038/nature07174>, 2008.
- 1184 Liu, J., Yuan, C., Hu, G. and Li, F.: Effects of light intensity on the growth and lipid accumulation of microalga *Scenedesmus*
1185 sp. 11-1 under nitrogen limitation, *Appl. Biochem. Biotechnol.*, 166(8), 2127–2137, doi:10.1007/s12010-012-9639-2,
1186 2012.
- 1187 Liu, B.: Biochemical Characterization of Triacylglycerol Metabolism in Microalgae, PhD thesis, Biochemistry and Molecular
1188 Biology, Michigan State University, USA. pp. 165, ISBN: 97813037151741303715171, 2014.
- 1189 Loh, A. N., Bauer, J. E. and Druffel, E. R. M.: Variable ageing and storage of dissolved organic components in the open ocean,
1190 *Nature*, 430(7002), 877–881, doi:10.1038/nature02780, 2004.
- 1191 Luan, J., Zhang, C., Xu, B., Xue, Y., Ren, Y.: The predictive performances of random forest models with limited sample size
1192 and different species traits. *Fish. Res.* 227: 105534, <https://doi.org/10.1016/j.fishres.2020.105534>, 2020.
- 1193 Lyon, B. R. and
1194 Mock, T.: Polar microalgae: New approaches towards understanding adaptations to an extreme and changing
1195 environment, *Biology (Basel)*, 3(1), 56–80, doi:10.3390/biology3010056, 2014.
- 1195 Mackey, M. D., Mackey, D. J., Higgins, H. W. and Wright, S. W.: CHEMTAX - A program for estimating class abundances
1196 from chemical markers: Application to HPLC measurements of phytoplankton, *Mar. Ecol. Prog. Ser.*, 144(1–3), 265–
1197 283, doi:10.3354/meps144265, 1996.
- 1198 Masuda, S., Kobayashi, M., Icochea Salas, L.A. and Rosales Quintana, G.M.: Possible link between temperatures in the
1199 seashore and open ocean waters of Peru identified by using new seashore water data. *Progr. Earth Planet. Sci.*, 10, 38,
1200 <https://doi.org/10.1186/s40645-023-00571-1>, 2023.
- 1201 Meador, T. B., Goldenstein, N. I., Gogou, A., Herut, B., Psarra, S., Tsagaraki, T. M. and Hinrichs, K. U.: Planktonic lipidome
1202 responses to Aeolian dust input in low-biomass oligotrophic marine mesocosms, *Front. Mar. Sci.*, 4(APR), 1–20,
1203 doi:10.3389/fmars.2017.00113, 2017.
- 1204 Messié, M., Ledesma, J., Kolber, D. D., Michisaki, R. P., Foley, D. G., & Chavez, F. P.: Potential new production estimates
1205 in four eastern boundary upwelling ecosystems. *Progress in Oceanography*, 83(1-4), 151-158, doi:
1206 <https://doi.org/10.1016/j.pocean.2009.07.018>, 2009.

- 1207 Messié, M. and Chavez, F. P.: Seasonal regulation of primary production in eastern boundary upwelling systems, *Prog.*
1208 *Oceanogr.*, 134, 1–18, doi:10.1016/j.pocean.2014.10.011, 2015.
- 1209 Meyer, J., Löscher, C. R., Lavik, G. and Riebesell, U.: Mechanisms of P* reduction in the eastern tropical South Pacific, *Front.*
1210 *Mar. Sci.*, 4(JAN), 1–12, doi:10.3389/fmars.2017.00001, 2017.
- 1211 Meyers, M. T., Cochlan, W. P., Carpenter, E. J. and Kimmerer, W. J.: Effect of ocean acidification on the nutritional quality
1212 of marine phytoplankton for copepod reproduction, *PLoS One*, 14(5), 1–22, doi:10.1371/journal.pone.0217047, 2019.
- 1213 Mimouni, V., Couzinet-Mossion, A., Ulmann, L., & Wielgosz-Collin, G.: Lipids from microalgae. In: Levine, I. A., Fleurence,,
1214 J. (Eds) *Microalgae in health and disease prevention*, pp. 109-131, Academic Press, doi: 10.1016/B978-0-12-811405-
1215 6.00005-0, 2018.
- 1216 Min, M.A., Needham, D.M., Sudek, S., Truelove, N.K., Pitz, K.J., Chavez, G.M., Poirier, C., Gardeler, B., von der Esch, E.,
1217 Ludwig, A., Riebesell, U., Worden, A.Z., Chavez, F.P., 2023. Ecological divergence of a mesocosm in an eastern
1218 boundary upwelling system assessed with multi-marker environmental DNA metabarcoding. *Biogeosciences* 20, 1277–
1219 1298. <https://doi.org/10.5194/bg-20-1277-2023>, 2023.
- 1220 Moazami-Goudarzi, M. and Colman, B.: Changes in carbon uptake mechanisms in two green marine algae by reduced seawater
1221 pH, *J. Exp. Mar. Bio. Ecol.*, 413, 94–99, doi:10.1016/j.jembe.2011.11.017, 2012.
- 1222 Mock, T. and Gradinger, R.: Changes in photosynthetic carbon allocation in algal assemblages of Arctic sea ice with
1223 decreasing nutrient concentrations and irradiance, *Mar. Ecol. Prog. Ser.*, 202, 1–11, doi:10.3354/meps202001, 2000.
- 1224 Morales, M., Aflalo, C. and Bernard, O.: Microalgal lipids: A review of lipids potential and quantification for 95 phytoplankton
1225 species, *Biomass and Bioenergy*, 150(April), 106108, doi:10.1016/j.biombioe.2021.106108, 2021.
- 1226 Morán, X. A. G., López-Urrutia, Á., Calvo-Díaz, A. and LI, W. K. W.: Increasing importance of small phytoplankton in a
1227 warmer ocean, *Glob. Chang. Biol.*, 16(3), 1137–1144, doi:10.1111/j.1365-2486.2009.01960.x, 2010.
- 1228 Moran, M. A. and Durham, B. P.: Sulfur metabolites in the pelagic ocean, *Nat. Rev. Microbiol.*, 17(11), 665–678,
1229 doi:10.1038/s41579-019-0250-1, 2019.
- 1230 Morris, A. W. and Riley, J. P.: The determination of nitrate in sea water, *Anal. Chim. Acta*, 29(C), 272–279,
1231 doi:10.1016/S0003-2670(00)88614-6, 1963.
- 1232 Mullin, J. B. and Riley, J. P.: The colorimetric determination of silicate with special reference to sea and natural waters, *Anal.*
1233 *Chim. Acta*, 12(C), 162–176, doi:10.1016/S0003-2670(00)87825-3, 1955.
- 1234 Murphy, J. and Riley, J. P.: A modified single solution method for the determination of phosphate in natural waters, *Anal.*
1235 *Chim. Acta*, 27(C), 31–36, doi:10.1016/S0003-2670(00)88444-5, 1962.
- 1236 Myklestad, S. M.: Dissolved Organic Carbon from Phytoplankton, In Wangersky, P. J., (Eds) *Marine Chemistry. The*
1237 *Handbook of Environmental Chemistry*, Springer, Berlin, Heidelberg, 111–148, doi:10.1007/10683826_5, 2000.
- 1238 Nakajima, Y., Umena, Y., Nagao, R., Endo, K., Kobayashi, K., Akita, F., Suga, M., Wada, H., Noguchi, T., and Shen, J. R.,
1239 Thylakoid membrane lipid sulfoquinovosyl-diacylglycerol (SQDG) is required for full functioning photosystem II in

- 1240 Thermosynechococcus elongatus, *J. Biol. Chem.*, 293, 14786-14797, <https://doi.org/10.1074/jbc.RA118.004304d>,
1241 2018.
- 1242 Naqvi, S. W. A., Bange, H., Farias, L., Monteiro, P., Scranton, M., & Zhang, J.: Marine hypoxia/anoxia as a source of CH₄
1243 and N₂O. *Biogeosciences*, 7, <https://doi.org/10.5194/bg-7-2159>, 2010. Nebbioso, A. and Piccolo, A.: Molecular
1244 characterization of dissolved organic matter (DOM): A critical review, *Anal. Bioanal. Chem.*, 405(1), 109–124,
1245 doi:10.1007/s00216-012-6363-2, 2013.
- 1246 Neidleman, S. L.: Effects of temperature on lipid unsaturation, *Biotechnol. Genet. Eng. Rev.*, 5(1), 245–268,
1247 doi:10.1080/02648725.1987.10647839, 1987.
- 1248 Orcutt, D. M. and Patterson, G. W.: Effect of light intensity upon lipid composition of *Nitzschia closterium* (*Cylindrotheca*
1249 *fusiformis*), *Lipids*, 9(12), 1000–1003, doi:10.1007/BF02533825, 1974.
- 1250 Oyarzún, D. and Brierley, C. M.: The future of coastal upwelling in the Humboldt current from model projections, *Clim.*
1251 *Dynam.*, 52, 599–615, <https://doi.org/10.1007/s00382-018-4158-7>, 2019.
- 1252 Pal, D., Khozin-Goldberg, I., Cohen, Z. and Boussiba, S.: The effect of light, salinity, and nitrogen availability on lipid
1253 production by *Nannochloropsis* sp., *Appl. Microbiol. Biotechnol.*, 90(4), 1429–1441, doi:10.1007/s00253-011-3170-1,
1254 2011.
- 1255 Paul, A. J., Bach, L. T., Schulz, K. G., Boxhammer, T., Czerny, J., Achterberg, E. P., Hellemann, D., Trense, Y., Nausch, M.,
1256 Sswat, M. and Riebesell, U.: Effect of elevated CO₂ on organic matter pools and fluxes in a summer Baltic Sea plankton
1257 community, *Biogeosciences*, 12(20), 6181–6203, doi:10.5194/bg-12-6181-2015, 2015.
- 1258 Peng, X., Liu, S., Zhang, W., Zhao, Y., Chen, L., Wang, H. and Liu, T.: Triacylglycerol accumulation of *Phaeodactylum*
1259 *tricornutum* with different supply of inorganic carbon, *J. Appl. Phycol.*, 26(1), 131–139, doi:10.1007/s10811-013-0075-
1260 7, 2014.
- 1261 Pitcher, G. C., Aguirre-Velarde, A., Breitburg, D., Cardich, J., Carstensen, J., Conley, D. J., Dewitte, B., Engel, A.,
1262 EspinozaMorriberón, D., Flores, G., Garçon, V., Graco, M., Grégoire, M., Gutiérrez, D., Hernandez-Ayon, J. M., Huang,
1263 H.-H. M., Isensee, K., Jacinto, M. E., Levin, L., Lorenzo, A., Machu, E., Merma, L., Montes, I., Swa, N., Paulmier, A.,
1264 Roman, M., Rose, K., Hood, R., Rabalais, N. N., Salvanes, A. G. V., Salvatelli, R., Sánchez, S., Sifeddine, A., Tall, A.
1265 W., Plas, A. K. v. d., Yasuhara, M., Zhang, J., and Zhu, Z. Y.: System controls of coastal and open ocean oxygen
1266 depletion, *Prog. Oceanogr.*, 197, 102613, <https://doi.org/10.1016/j.pcean.2021.102613>, 2021.
- 1267 Poerschmann, J., Spijkerman, E. and Langer, U.: Fatty acid patterns in *Chlamydomonas* sp. as a marker for nutritional regimes
1268 and temperature under extremely acidic conditions, *Microb. Ecol.*, 48(1), 78–89, doi:10.1007/s00248-003-0144-6, 2004.
- 1269 Popenoerf, K.J., Lomas, M.W. and Van Mooy, B.A.: Microbial sources of intact polar diacylglycerolipids in the Western
1270 North Atlantic Ocean. *Organic geochemistry*, 42(7), pp.803-811, <https://doi.org/10.1016/j.orggeochem.2011.05.003>,
1271 2011.
- 1272 Popko, J., Herrfurth, C., Feussner, K., Ischebeck, T., Iven, T., Haslam, R., Hamilton, M., Sayanova, O., Napier, J., Khozin-
1273 Goldberg, I. and Feussner, I.: Metabolome analysis reveals betaine lipids as major source for triglyceride formation, and

1274 the accumulation of sedoheptulose during nitrogen-starvation of *Phaeodactylum tricornutum*, *PLoS One*, 11(10), 1–23,
1275 doi:10.1371/journal.pone.0164673, 2016.

1276 Raven, J. A., and Beardall, J.: Carbohydrate metabolism and respiration in algae, In Larkum, A. W. D., Douglas, S. S., Raven,
1277 J. A. (Eds) *Photosynthesis in algae*, 14, pp. 205-224, Springer, Dordrecht, [https://doi.org/10.1007/978-94-007-1038-](https://doi.org/10.1007/978-94-007-1038-2_10)
1278 [2_10](https://doi.org/10.1007/978-94-007-1038-2_10), 2003.

1279 Riebesell, U., Czerny, J., Von Bröckel, K., Boxhammer, T., Büdenbender, J., Deckelnick, M., Fischer, M., Hoffmann, D.,
1280 Krug, S. A., Lentz, U., Ludwig, A., Mucbe, R. and Schulz, K. G.: Technical Note: A mobile sea-going mesocosm system
1281 - New opportunities for ocean change research, *Biogeosciences*, 10(3), 1835–1847, doi:10.5194/bg-10-1835-2013, 2013.

1282 Roessler, P. G. Environmental control of glycerolipid metabolism in microalgae: commercial implications and future research
1283 directions, *Journal of Phycology*, 26.3, 393-399, <https://doi.org/10.1111/j.0022-3646.1990.00383.x>, 1990.

1284 Russell, N. J., and Nichols, D. S.: Polyunsaturated fatty acids in marine bacteria—a dogma rewritten, *Microbiology*, 145.4,
1285 767-779, doi:10.1099/13500872-145-4-767, 1999.

1286 Rütters, H., Sass, H., Cypionka, H., and Rullkötter, J.: Monoalkylether phospholipids in the sulfate-reducing bacteria
1287 *Desulfosarcina variabilis* and *Desulforhabdus amnigenus*, *Arch. Microbiol.*, 176, 435–442, doi:
1288 10.1007/s002030100343, 2001.

1289 Sakamoto, T. and Murata, N.: Regulation of the desaturation of fatty acids and its role in tolerance to cold and salt stress, *Curr.*
1290 *Opin. Microbiol.*, 5(2), 206–210, doi:10.1016/S1369-5274(02)00306-5, 2002.

1291 Sakurai, I., Hagio, M., Gombos, Z., Tyystjärvi, T., Paakkarinen, V., Aro, E. M. and Wada, H.: Requirement of
1292 Phosphatidylglycerol for Maintenance of Photosynthetic Machinery, *Plant Physiol.*, 133(3), 1376–1384,
1293 doi:10.1104/pp.103.026955, 2003.

1294 Sato, N. and Murata, N.: Temperature shift-induced responses in lipids in the blue-green alga, *Anabaena variabilis*, *Biochim.*
1295 *Biophys. Acta - Lipids Lipid Metab.*, 619(2), 353–366, doi:10.1016/0005-2760(80)90083-1, 1980.

1296 Sato, N., Aoki, M., Maru, Y., Sonoike, K., Minoda, A. and Tsuzuki, M.: Involvement of sulfoquinovosyl diacylglycerol in the
1297 structural integrity and heat-tolerance of photosystem II, *Planta*, 217(2), 245–251, doi:10.1007/s00425-003-0992-9,
1298 2003.

1299 Sayanova, O., Mimouni, V., Ulmann, L., Morant-Manceau, A., Pasquet, V., Schoefs, B. and Napier, J. A.: Modulation of lipid
1300 biosynthesis by stress in diatoms, *Philos. Trans. R. Soc. B Biol. Sci.*, 372(1728), doi:10.1098/rstb.2016.0407, 2017.

1301 Schubotz, F., Wakeham, S. G., Lipp, J. S., Fredricks, H. F. and Hinrichs, K. U.: Detection of microbial biomass by intact polar
1302 membrane lipid analysis in the water column and surface sediments of the Black Sea, *Environ. Microbiol.*, 11(10), 2720–
1303 2734, doi:10.1111/j.1462-2920.2009.01999.x, 2009.

1304 Schubotz, F., Xie, S., Lipp, J. S., Hinrichs, K. and Wakeham, S. G.: Intact polar lipids in the water column of the eastern
1305 tropical North Pacific: abundance and structural variety of non-phosphorus lipids, *Biogeosciences*, 15, 6481-6501,
1306 <https://doi.org/10.5194/bg-15-6481-2018>, 2018.

1307 Sinensky, M.: Homeoviscous adaptation: a homeostatic process that regulates the viscosity of membrane lipids in *Escherichia*
1308 *coli*, *Proc. Natl. Acad. Sci. U. S. A.*, 71(2), 522–525, doi:10.1073/pnas.71.2.522, 1974.

1309 Singh, Y. and Kumar, H. D.: Lipid and hydrocarbon production by *Botryococcus* spp. under nitrogen limitation and
1310 anaerobiosis, *World J. Microbiol. Biotechnol.*, 8(2), 121–124, doi:10.1007/BF01195829, 1992.

1311 Smalley, G. W., Coats, D. W., and Stoecker, D. K.: Feeding in the mixotrophic dinoflagellate *Ceratium furca* is influenced by
1312 intracellular nutrient concentrations, *Mar. Ecol. Prog. Ser.*, 262, 137–151, doi:10.3354/meps262137, 2003.

1313 Speciale, G., Jin, Y., Davies, G. J., Williams, S. J. and Goddard-Borger, E. D.: YihQ is a sulfoquinovosidase that cleaves
1314 sulfoquinovosyl diacylglyceride sulfolipids, *Nat. Chem. Biol.*, 12(4), 215–217, doi:10.1038/nchembio.2023, 2016.

1315 Stramma, L., Johnson, G. C., Sprintall, J. and Mohrholz, V.: Expanding oxygen-minimum zones in the tropical oceans, *Science*
1316 , 320, 655–658, doi:10.1126/science.1153847, 2008.

1317 Stramma, L., Schmidtko, S., Levin, L. A. and Johnson, G. C.: Ocean oxygen minima expansions and their biological impacts,
1318 *Deep. Res. Part I Oceanogr. Res. Pap.*, 57(4), 587–595, doi:10.1016/j.dsr.2010.01.005, 2010.

1319 Sturt, H. F., Summons, R. E., Smith, K., Elvert, M. and Hinrichs, K. U.: Intact polar membrane lipids in prokaryotes and
1320 sediments deciphered by high-performance liquid chromatography/electrospray ionization multistage mass spectrometry
1321 - New biomarkers for biogeochemistry and microbial ecology, *Rapid Commun. Mass Spectrom.*, 18(6), 617–628,
1322 doi:10.1002/rcm.1378, 2004.

1323 Sukenik, A., Zmora, O. and Carmeli, Y.: Biochemical quality of marine unicellular algae with special emphasis on lipid
1324 composition. II. *Nannochloropsis* sp., *Aquaculture*, 117(3–4), 313–326, doi:10.1016/0044-8486(93)90328-V, 1993.

1325 Suzumura, M.: Phospholipids in marine environments: a review, *Talanta*, 66, 422–434, doi: 10.1016/j.talanta.2004.12.008,
1326 2005.

1327 Tatsuzawa, H. and Takizawa, E.: Fatty Acid and Lipid Composition of the Acidophilic green alga *Chlamydomonas* Sp., *Journal*
1328 *of Phycology*, 32(4), 598–601, <https://doi.org/10.1111/j.0022-3646.1996.00598.x>, 1996.

1329 Taucher, J., Bach, L. T., Boxhammer, T., Nauendorf, A., Achterberg, E. P., Algueró-Muñiz, M., Arístegui, J., Czerny, J.,
1330 Esposito, M., Guan, W., Haunost, M., Horn, H. G., Ludwig, A., Meyer, J., Spisla, C., Sswat, M., Stange, P., Riebesell,
1331 U., Aberle-Malzahn, N., Archer, S., Boersma, M., Broda, N., Büdenbender, J., Clemmesen, C., Deckelnick, M., Dittmar,
1332 T., Dolores-Gelado, M., Dörner, I., Fernández-Urruzola, I., Fiedler, M., Fischer, M., Fritsche, P., Gomez, M., Grossart,
1333 H. P., Hattich, G., Hernández-Brito, J., Hernández-Hernández, N., Hernández-León, S., Hornick, T., Kolzenburg, R.,
1334 Krebs, L., Kreuzburg, M., Lange, J. A. F., Lischka, S., Linsenbarth, S., Löscher, C., Martínez, I., Montoto, T., Nachtigall,
1335 K., Osma-Prado, N., Packard, T., Pansch, C., Posman, K., Ramírez-Bordón, B., Romero-Kutzner, V., Rummel, C., Salta,
1336 M., Martínez-Sánchez, I., Schröder, H., Sett, S., Singh, A., Suffrian, K., Tames-Espinosa, M., Voss, M., Walter, E.,
1337 Wannicke, N., Xu, J. and Zark, M.: Influence of ocean acidification and deep water upwelling on oligotrophic plankton
1338 communities in the subtropical North Atlantic: Insights from an in situ mesocosm study, *Front. Mar. Sci.*, 4(APR),
1339 doi:10.3389/fmars.2017.00085, 2017.

- 1340 Thamdrup, B., Dalsgaard, T. and Revsbech, N. P.: Widespread functional anoxia in the oxygen minimum zone of the Eastern
1341 South Pacific, *Deep. Res. Part I Oceanogr. Res. Pap.*, 65, 36–45, doi:10.1016/j.dsr.2012.03.001, 2012.
- 1342 Tréguer, P., Bowler, C., Moriceau, B., Dutkiewicz, S., Gehlen, M., Aumont, O., Bittner, L., Dugdale, R., Finkel, Z., Iudicone,
1343 D., Jahn, O., Guidi, L., Lasbleiz, M., Leblanc, K., Levy, M., and Pondaven, P.: Influence of diatom diversity on the
1344 ocean biological carbon pump. *Nature Geosci*, 11, 27–37, doi: <https://doi.org/10.1038/s41561-017-0028-x>, 2018.
- 1345 Tretkoff, E. Research Spotlight: Coastal cooling and marine productivity increasing off Peru. *Eos Transact. Am. Geophys.*
1346 *Union* 92, 184–184. doi: 10.1029/2011eo210009, 2011
- 1347 Twining, C. W., Taipale, S. J., Ruess, L., Bec, A., Martin-Creuzburg, D. and Kainz, M. J.: Stable isotopes of fatty acids:
1348 Current and future perspectives for advancing trophic ecology, *Philos. Trans. R. Soc. B Biol. Sci.*, 375(1804),
1349 doi:10.1098/rstb.2019.0641, 2020.
- 1350
- 1351 Tyrallis, H., Papacharalampous, G., & Langousis, A. A brief review of random forests for water scientists and practitioners and
1352 their recent history in water resources. *Water*, 11(5), 910, <https://doi.org/10.3390/w11050910>, 2019.
- 1353 Ulloa, O. and Pantoja, S.: The oxygen minimum zone of the eastern South Pacific, *Deep. Res. Part II Top. Stud. Oceanogr.*,
1354 56(16), 987–991, doi:10.1016/j.dsr2.2008.12.004, 2009.
- 1355 Van Mooy, B. A. S. and Fredricks, H. F.: Bacterial and eukaryotic intact polar lipids in the eastern subtropical South Pacific:
1356 Water-column distribution, planktonic sources, and fatty acid composition, *Geochim. Cosmochim. Acta*, 74(22), 6499–
1357 6516, doi:10.1016/j.gca.2010.08.026, 2010.
- 1358 Van Mooy, B. A. S., Fredricks, H. F., Pedler, B. E., Dyhrman, S. T., Karl, D. M., Koblížek, M., Lomas, M. W., Mincer, T. J.,
1359 Moore, L. R., Moutin, T., Rappé, M. S. and Webb, E. A.: Phytoplankton in the ocean use non-phosphorus lipids in
1360 response to phosphorus scarcity, *Nature*, 458(7234), 69–72, doi:10.1038/nature07659, 2009.
- 1361 Van Mooy, B. A., Rocap, G., Fredricks, H. F., Evans, C. T., and Devol, A. H.: Sulfolipids dramatically decrease phosphorus
1362 demand by picocyanobacteria in oligotrophic marine environments, *P. Natl. Acad. Sci. USA*, 103(23), 8607–8612,
1363 <https://doi.org/10.1073/pnas.0600540103>, 2006.
- 1364 Vargas, C. A., Cantarero, S. I., Sepúlveda, J. A., Galán, A., De Pol Holz, R., Walker, B., Schneider, W., Farías, L., Cornejo
1365 D’Ottone, M., Walker, J., Xu, X., and Salisbury, J.: A source of isotopically light organic carbon in a low-pH anoxic
1366 marine zone. *Nature Communications*, 12, 1604. <https://doi.org/10.1038/s41467-021-21871-4>, 2021. Volkman, J. K.,
1367 Jeffrey, S. W., Nichols, P. D., Rogers, G. I. and Garland, C. D.: Fatty acid and lipid composition of 10 species of
1368 microalgae used in mariculture, *J. Exp. Mar. Bio. Ecol.*, 128(3), 219–240, doi:10.1016/0022-0981(89)90029-4, 1989.
- 1369 Volkman, J. K., Barrett, S. M., Blackburn, S. I., Mansour, M. P., Sikes, E. L. and Gelin, F.: Microalgal biomarkers: A review
1370 of recent research developments, *Org. Geochem.*, 29(5-7-7 pt 2), 1163–1179, doi:10.1016/S0146-6380(98)00062-X,
1371 1998.
- 1372 Wada, H., and Murata, N.: Lipids in thylakoid membranes and photosynthetic cells, In: *Lipids in Photosynthesis*, Springer,
1373 Dordrecht, 1-9, https://doi.org/10.1007/978-90-481-2862-1_1, 2009.

- 1374 Wagner, S., Schubotz, F., Kaiser, K., Hallmann, C., Waska, H., Rossel, P. E., Hansman, R., Elvert, M., Middelburg, J. J.,
1375 Engel, A., Blattmann, T. M., Catalá, T. S., Lennartz, S. T., Gomez-Saez, G. V., Pantoja-Gutiérrez, S., Bao, R. and Galy,
1376 V.: Soothsaying DOM: A Current Perspective on the Future of Oceanic Dissolved Organic Carbon, *Front. Mar. Sci.*,
1377 7(May), 1–17, doi:10.3389/fmars.2020.00341, 2020.
- 1378 Wakeham, S. G., Turich, C., Schubotz, F., Podlaska, A., Li, X. N., Varela, R., Astor, Y., Sáenz, J. P., Rush, D., Sinninghe
1379 Damsté, J. S., Summons, R. E., Scranton, M. I., Taylor, G. T. and Hinrichs, K. U.: Biomarkers, chemistry and
1380 microbiology show chemoautotrophy in a multilayer chemocline in the Cariaco Basin, *Deep. Res. Part I Oceanogr. Res.*
1381 *Pap.*, 63, 133–156, doi:10.1016/j.dsr.2012.01.005, 2012.
- 1382 Wang, X., Shen, Z. and Miao, X.: Nitrogen and hydrophosphate affects glycolipids composition in microalgae, *Sci. Rep.*,
1383 6(July), 1–9, doi:10.1038/srep30145, 2016.
- 1384 Wilhelm, C., Jungandreas, A., Jakob, T. and Goss, R.: Light acclimation in diatoms: From phenomenology to mechanisms,
1385 *Mar. Genomics*, 16(1), 5–15, doi:10.1016/j.margen.2013.12.003, 2014.
- 1386 Wörmer, L., Lipp, J. S., Schröder, J. M., Hinrichs, K. U.: Application of two new LC–ESI–MS methods for improved detection
1387 of intact polar lipids (IPLs) in environmental samples, *Org. Geochem.*, 59, 10–21,
1388 <https://doi.org/10.1016/j.orggeochem.2013.03.004>, 2013.
- 1389 Wörmer, L., Lipp, J. S., and Hinrichs, K. U.: Comprehensive analysis of microbial lipids in environmental samples through
1390 HPLC-MS protocols, in: *Hydrocarbon and lipid microbiology protocols*, Springer, Berlin, Heidelberg, 289–317,
1391 https://doi.org/10.1007/8623_2015_183, 2015.
- 1392 Wright, J. J., Konwar, K. M. and Hallam, S. J.: Microbial ecology of expanding oxygen minimum zones, *Nat. Rev. Microbiol.*,
1393 10(6), 381–394, doi:10.1038/nrmicro2778, 2012.
- 1394 Wu, R. S. S., Wo, K. T. and Chiu, J. M. Y.: Effects of hypoxia on growth of the diatom *Skeletonema costatum*, *J. Exp. Mar.*
1395 *Bio. Ecol.*, 420–421, 65–68, doi:10.1016/j.jembe.2012.04.003, 2012.
- 1396 Wyrтки, K.: The oxygen minima in relation to ocean circulation, *Deep. Res. Oceanogr. Abstr.*, 9(1–2), 11–23,
1397 doi:10.1016/0011-7471(62)90243-7, 1962.
- 1398 Yang, C., Boggasch, S., Haase, W. and Paulsen, H.: Thermal stability of trimeric light-harvesting chlorophyll a/b complex
1399 (LHCIIb) in liposomes of thylakoid lipids, *Biochim. Biophys. Acta - Bioenerg.*, 1757(12), 1642–1648,
1400 doi:10.1016/j.bbabi.2006.08.010, 2006.
- 1401 Yang, K. and Han, X.: Accurate quantification of lipid species by electrospray ionization mass spectrometry - Meets a key
1402 challenge in lipidomics, *Metabolites*, 1(1), 21–40, doi:10.3390/metabo1010021, 2011.
- 1403 Yang, W., Catalanotti, C., Wittkopp, T. M., Posewitz, M. C. and Grossman, A. R.: Algae after dark: Mechanisms to cope with
1404 anoxic/hypoxic conditions, *Plant J.*, 82(3), 481–503, doi:10.1111/tj.12823, 2015.
- 1405 Yeesang, C. and Cheirsilp, B.: Effect of nitrogen, salt, and iron content in the growth medium and light intensity on lipid
1406 production by microalgae isolated from freshwater sources in Thailand, *Bioresour. Technol.*, 102(3), 3034–3040,
1407 doi:10.1016/j.biortech.2010.10.013, 2011.

- 1408 Yoon, K., Han, D., Li, Y., Sommerfeld, M. and Hu, Q.: Phospholipid:Diacylglycerol acyltransferase is a multifunctional
 1409 enzyme involved in membrane lipid turnover and degradation while synthesizing triacylglycerol in the unicellular green
 1410 microalga *Chlamydomonas reinhardtii*, *Plant Cell*, 24(9), 3708–3724, doi:10.1105/tpc.112.100701, 2012.
- 1411 Yvon-Durocher, G., Allen, A. P., Cellamare, M., Dossena, M., Gaston, K. J., Leitao, M., Montoya, J. M., Reuman, D. C.,
 1412 Woodward, G. and Trimmer, M.: Five Years of Experimental Warming Increases the Biodiversity and Productivity of
 1413 Phytoplankton, *PLoS Biol.*, 13(12), 1–22, doi:10.1371/journal.pbio.1002324, 2015.
- 1414 Zienkiewicz, K., Du, Z. Y., Ma, W., Vollheyde, K. and Benning, C.: Stress-induced neutral lipid biosynthesis in microalgae
 1415 — Molecular, cellular and physiological insights, *Biochim. Biophys. Acta - Mol. Cell Biol. Lipids*, 1861(9), 1269–1281,
 1416 doi:10.1016/j.bbailip.2016.02.008, 2016.
- 1417 Zink K-G, Wilkes H, Disko U, Elvert M, Horsfield B. Intact phospholipids—microbial “life markers” in marine deep
 1418 subsurface sediments. *Org. Geochem*; 34: 755-769, [https://doi.org/10.1016/S0146-6380\(03\)00041-X](https://doi.org/10.1016/S0146-6380(03)00041-X), 2003.

1419 **Tables**

1420

1421 **Table 1: Concentration of inorganic nutrients ($\mu\text{mol/L}$), nutrient stoichiometry, and pH_T of the two batches of ODZ**
 1422 **water collected and added to the mesocosm experiment.**

1423

	Si(OH)_4	PO_4^{3-}	NO_2^-	NH_4^+	NO_3^-	N:P:Si	pH_T	Depth (m)
Station 1	17.4	2.6	0	0.3	0	0.1:1.0:6.7	7.47	30
Station 3	19.6	2.5	2.9	0.3	1.1	1.7:1.0:7.8	7.49	70

1424

1425 **Table 2: IPL classes included in this study and their respective acronyms.**

1426

IPL Headgroups	Acronym	IPL Classes
Sulfoquinovosyl	SQ	Glycolipid
Monogalactosyldiacylglycerol	MG	Glycolipid
Digalactosyldiacylglycerol	DG	Glycolipid
Phosphatidylglycerol	PG	Phospholipid
Phosphatidylethanolamine	PE	Phospholipid
Phosphatidylcholine	PC	Phospholipid
Diacylglyceryl trimethylhomoserine	DGTS	Betaine Lipid
Diacylglyceryl hydroxymethyl-trimethyl-beta-alanine	DGTA	Betaine Lipid
Diacylglyceryl carboxyhydroxymethylcholine	DGCC	Betaine Lipid

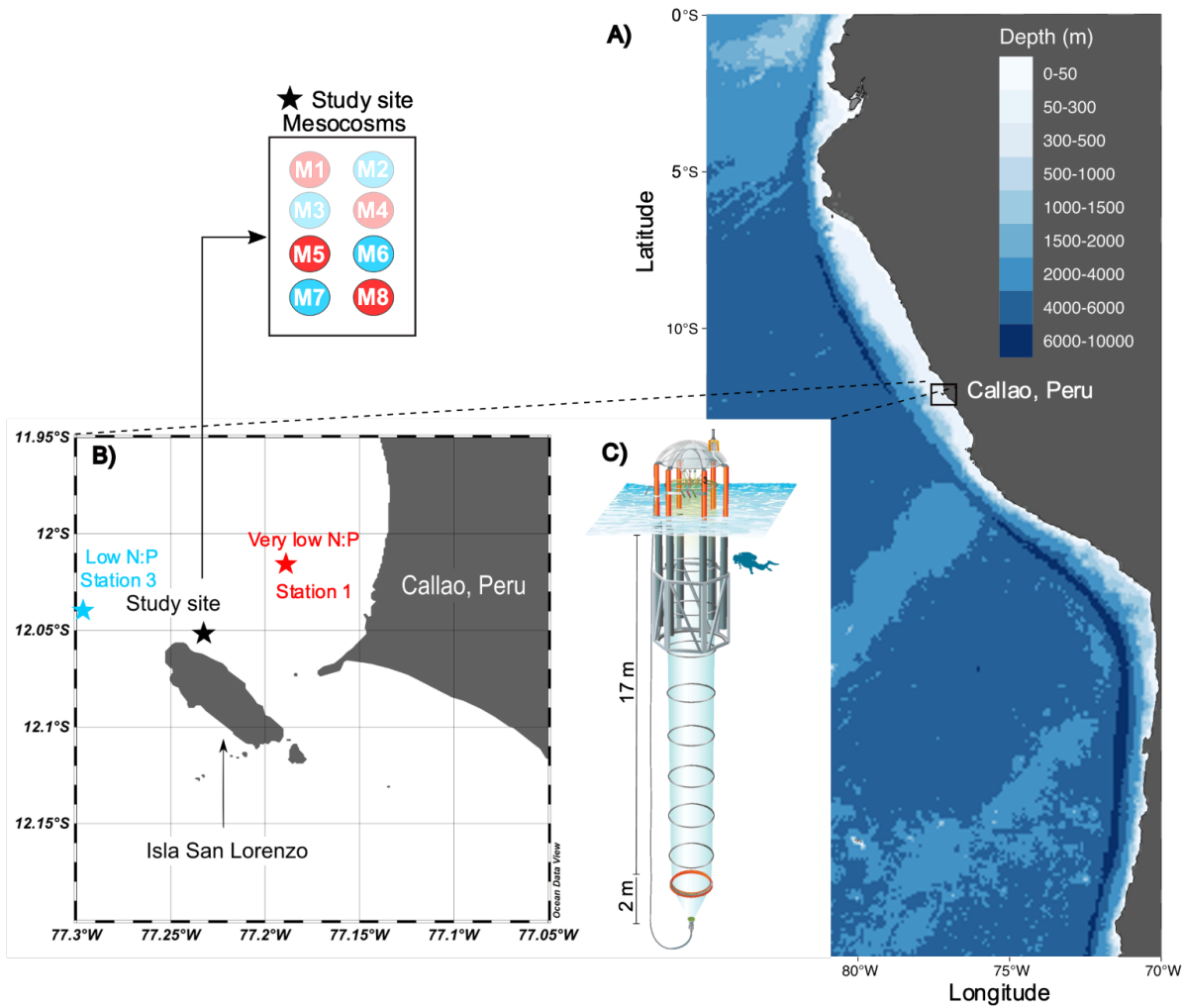
1427

1428

1429

1430 **Figures**

1431



1432

1433

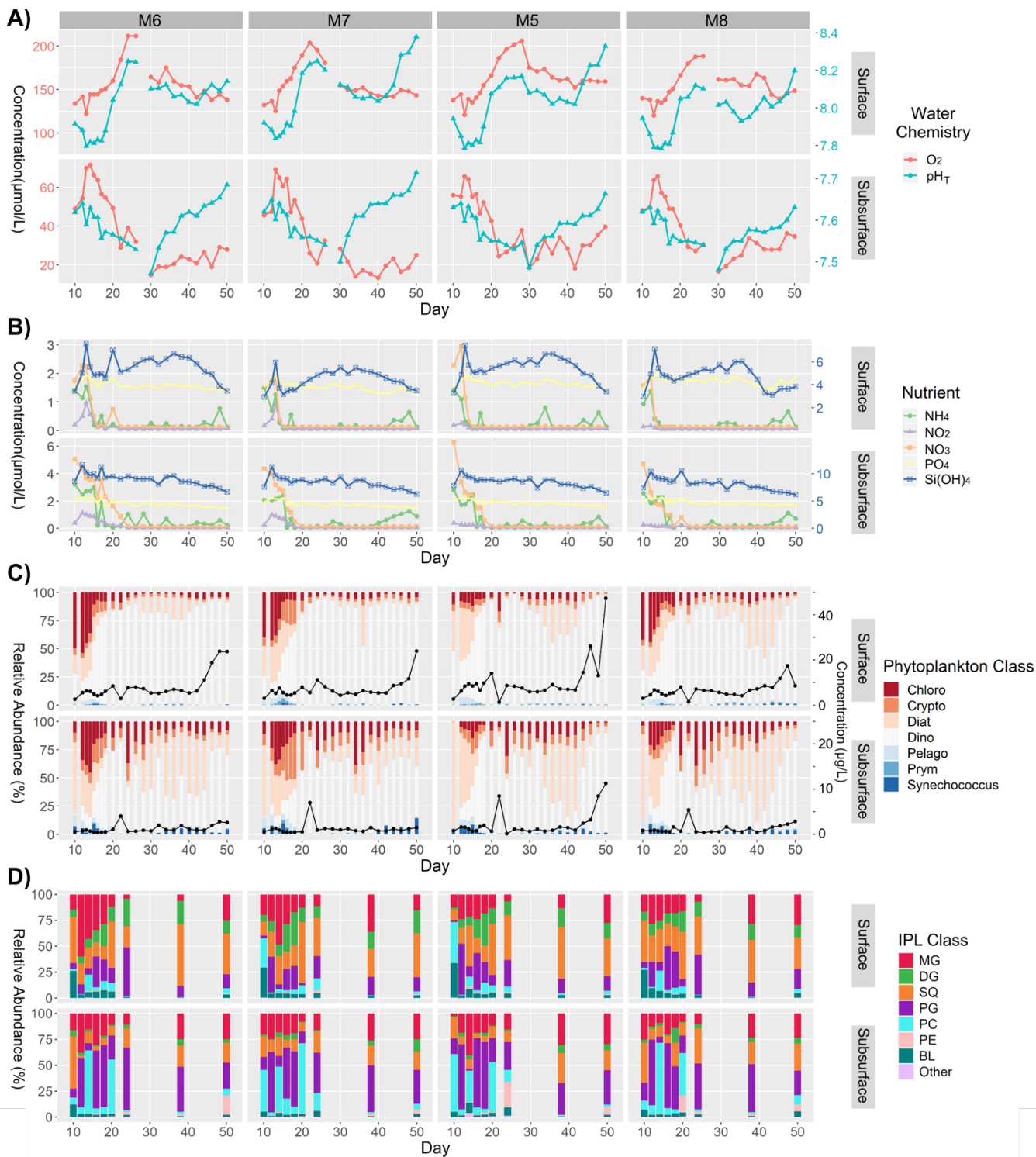
1434 **Figure 1: The KOSMOS study site. (A) Overview map indicating the location of the study region in La Punta, Callao, Perú. (B)**

1435 **Detailed map of the study site with the mesocosm arrangement (M1-8). Red (very low N:P) and blue (low N:P) colors indicate the**

1436 **different stations for ODZ water collection (1 and 3; star symbols) and replicates of the two different water treatments (numbers in**

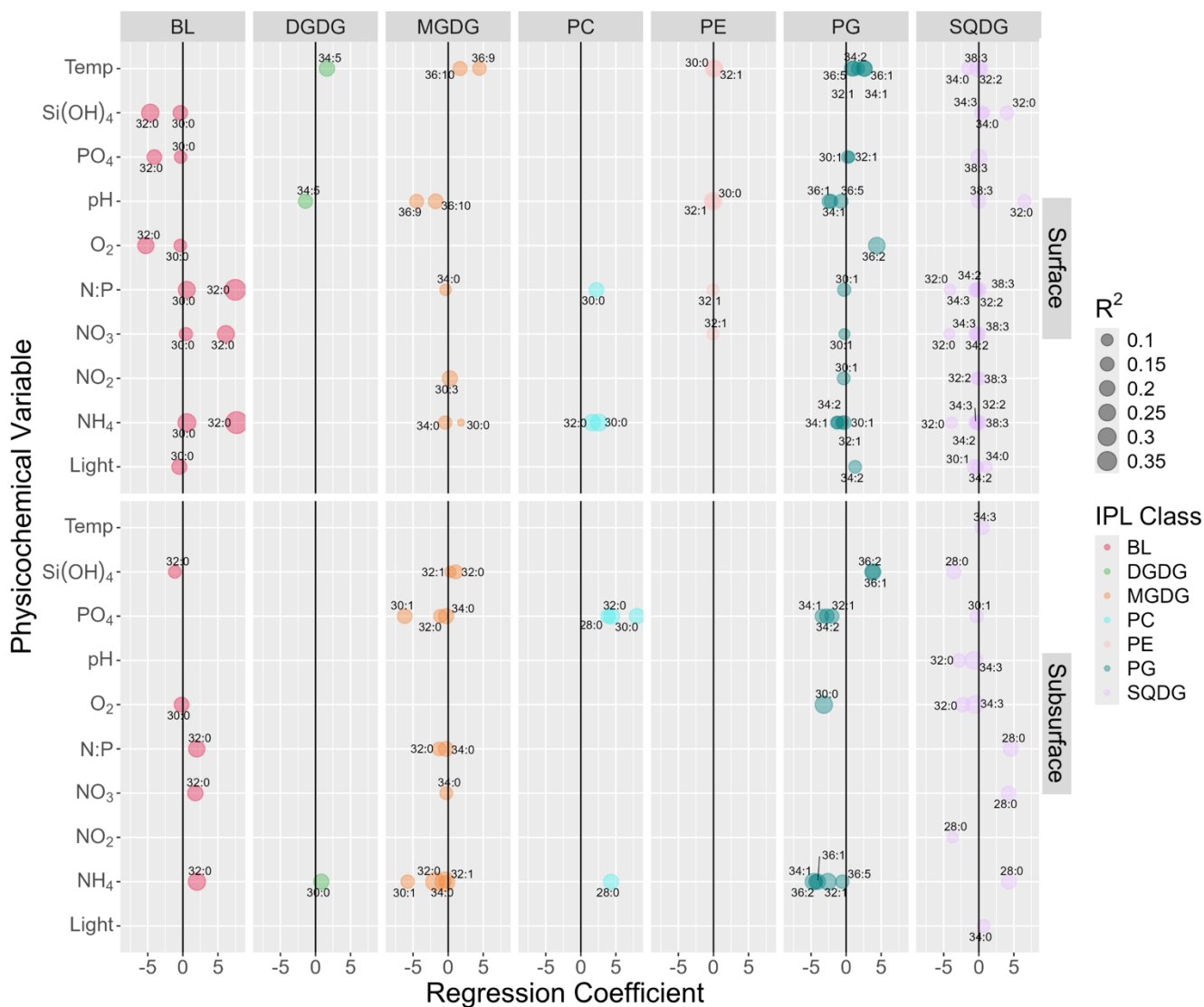
1437 **circles in insert). (C) Diagram of a mesocosm unit with underwater bag dimensions. Modified figure from Chen et al. (2022).**

1438



1440 **Figure 2: Summary of major physicochemical, biological, and lipidomic measurements in surface and subsurface waters of**
 1441 **mesocosms analyzed in this study from the time of deep-water injection to the end of the experiment. A) Concentration of O₂**
 1442 **($\mu\text{mol/L}$; left Y axis), and pH_T (total scale; right Y axis). B) Concentration of inorganic N (left Y axis), P (left Y axis), and Si(OH)₄**
 1443 **(right Y axis) expressed in $\mu\text{mol/L}$. C) Relative abundance (%) of phytoplankton classes (left Y axis) as well as total chl-a**
 1444 **concentrations expressed in $\mu\text{g/L}$ (black line; right Y axis). D) Relative abundance (%) of major IPL classes based on headgroup**
 1445 **contributions to the total IPL pool.**

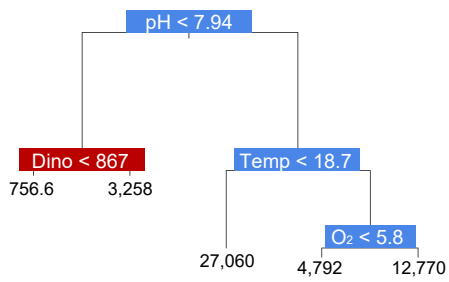
1446



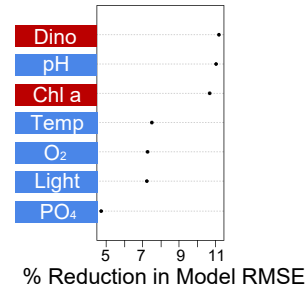
1447

1448 **Figure 3: Summary of multiple linear regression analysis between the abundances of major IPL molecules (> 2.5% of total IPL pool)**
 1449 **and physicochemical parameters showing only statistically significant ($p < 0.05$) linear responses after controlling for false discovery**
 1450 **rate using a 0.1 alpha cutoff on adjusted p-values. The size of circles indicates the magnitude of the linear regression adjusted R^2 .**
 1451 **The upper and lower panels represent surface and subsurface waters, respectively. Numbers next to circles indicate the total number**
 1452 **of carbon atoms and double bonds in core fatty acid chains.**

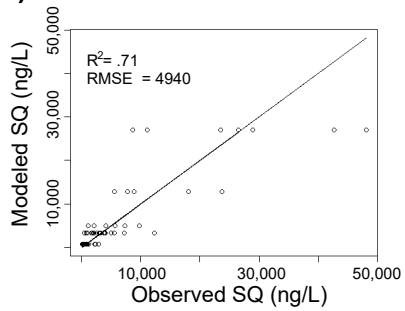
A) Pruned Tree SQ



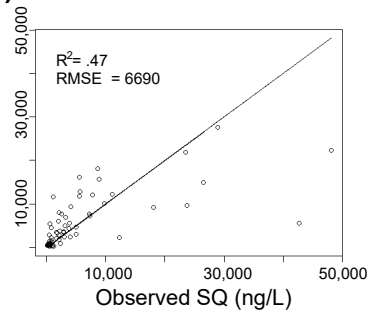
C) Random Forest SQ



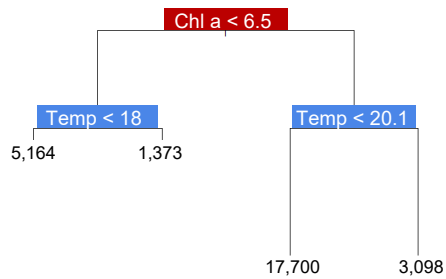
B)



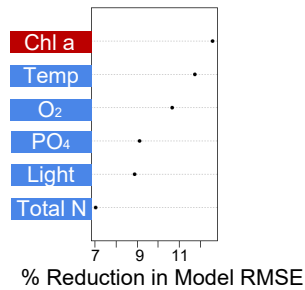
D)



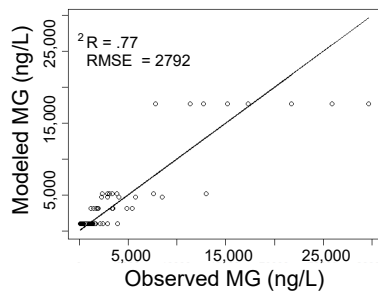
E) Pruned Tree MG



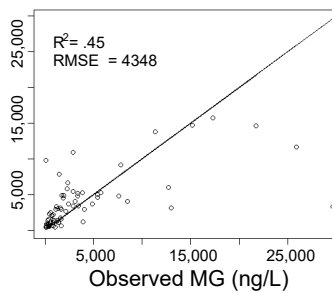
G) Random Forest MG



F)

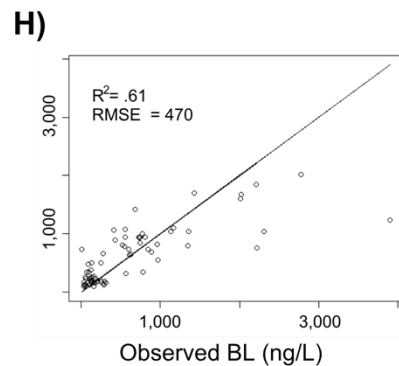
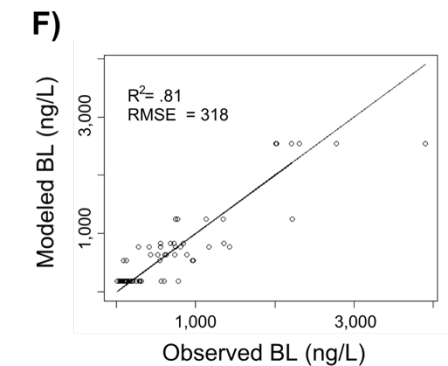
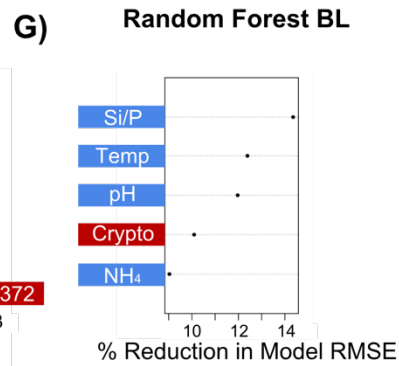
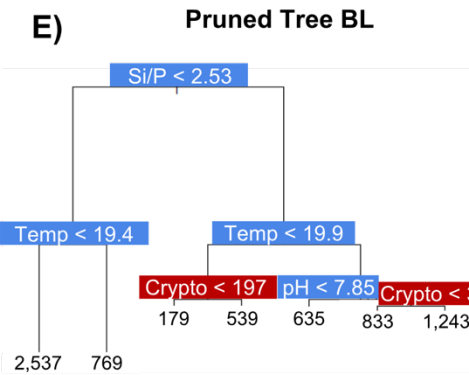
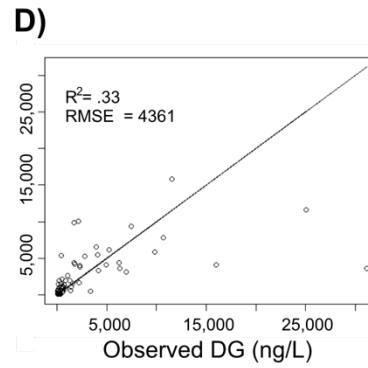
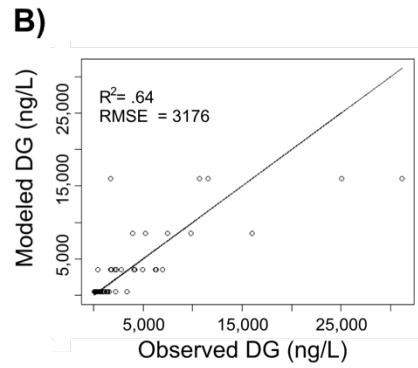
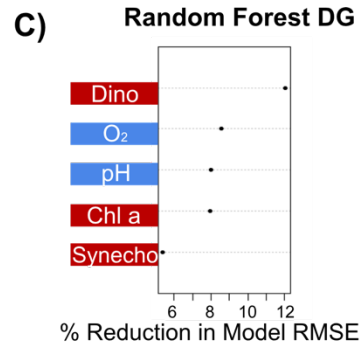
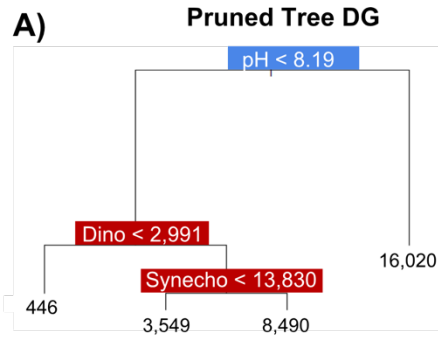


H)



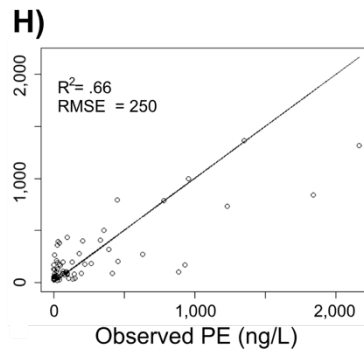
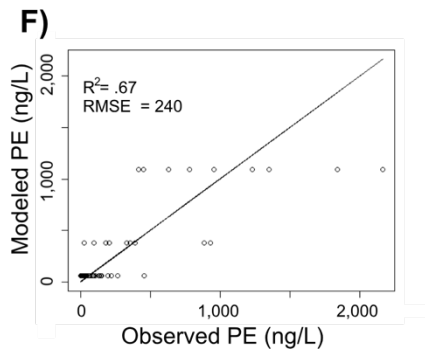
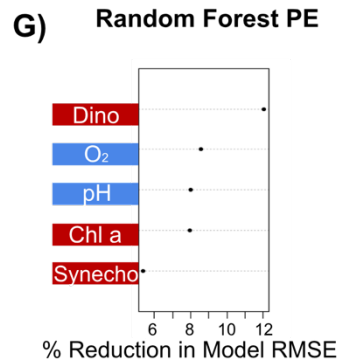
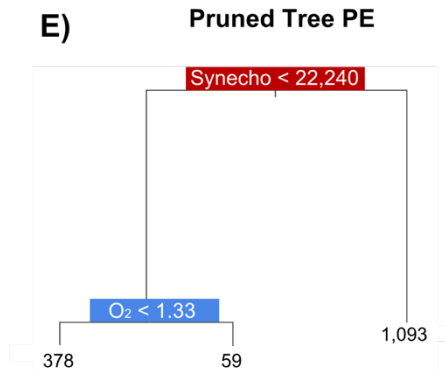
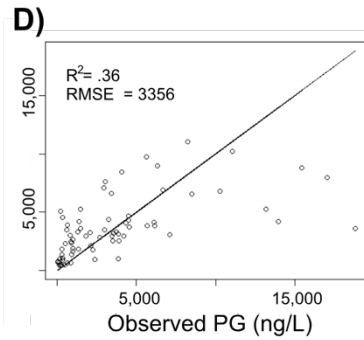
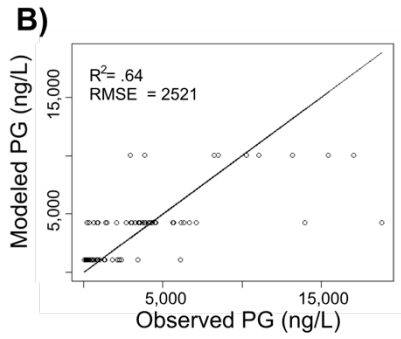
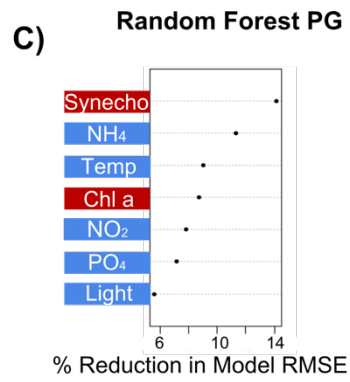
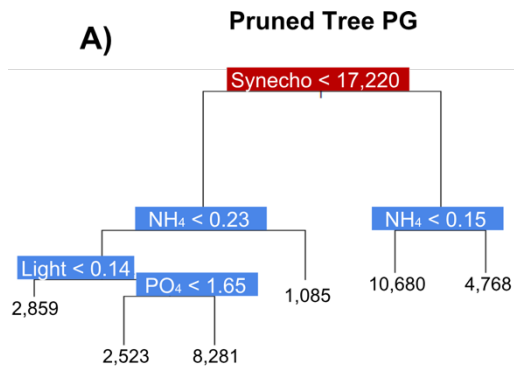
1454 **Figure 4: Classification and Regression Tree (CART) and Random Forest analyses of selected IPL classes (Top: SQ; Bottom: MG).**
1455 **A and E indicate a summary of primary predictors in the best fit CART (i.e. Pruned Tree), whereas B and F show model**
1456 **performance via adjusted R² and RMSE. C and G display Random Forest variable importance in the prediction of IPL classes as**
1457 **defined by % reduction in RMSE, whereas D and H show model performance via adjusted R² and RMSE. Environmental variables**
1458 **are depicted in blue, whereas biological variables are shown in red for both analyses.**

1459



1461 **Figure 5: Classification and Regression Tree (CART) and Random Forest analyses of selected IPL classes (Top: DG; Bottom: BL).**
1462 **A and E indicate a summary of primary predictors in the best fit CART (i.e. Pruned Tree), whereas B and F show model**
1463 **performance via adjusted R² and RMSE. C and G display Random Forest variable importance in the prediction of IPL classes as**
1464 **defined by % reduction in RMSE, whereas D and H show model performance via adjusted R² and RMSE. Environmental variables**
1465 **are depicted in blue, whereas biological variables are shown in red for both analyses.**

1466

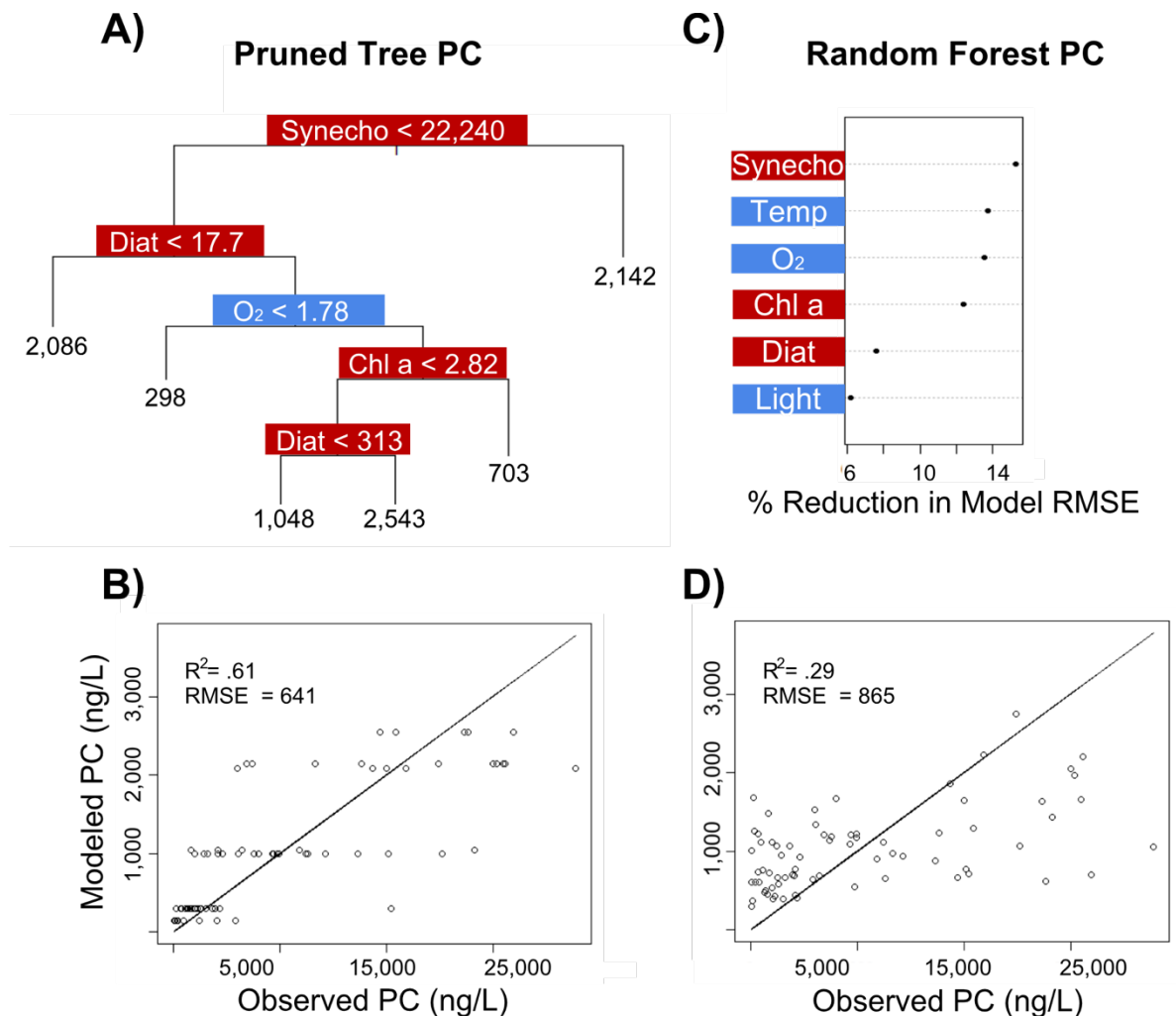


1468 **Figure 6: Classification and Regression Tree (CART) and Random Forest analyses of selected IPL classes (Top: PG; Bottom: PE).**
 1469 **A and E indicate a summary of primary predictors in the best fit CART (i.e. Pruned Tree), whereas B and F show model**
 1470 **performance via adjusted R² and RMSE. C and G display Random Forest variable importance in the prediction of IPL classes as**
 1471 **defined by % reduction in RMSE, whereas D and H show model performance via adjusted R² and RMSE. Environmental variables**
 1472 **are depicted in blue, whereas biological variables are shown in red for both analyses.**

1473

1474

1475



1476

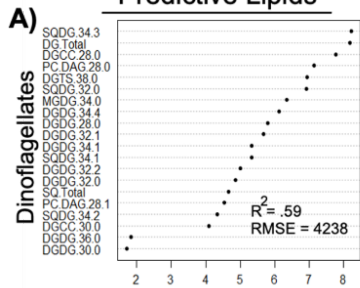
1477 **Figure 7: Classification and Regression Tree (CART) and Random Forest analyses of selected IPL classes (PC). A indicate a**
 1478 **summary of primary predictors in the best fit CART (i.e. Pruned Tree), whereas B shows model performance via adjusted R² and**
 1479 **RMSE. C and G display Random Forest variable importance in the prediction of IPL classes as defined by % reduction in RMSE,**
 1480 **whereas D show model performance via adjusted R² and RMSE. Environmental variables are depicted in blue, whereas biological**
 1481 **variables are shown in red for both analyses.**

1482

Predictive Lipids

Dominant IPL Classes

Potential IPL Remodeling



SQ, DG

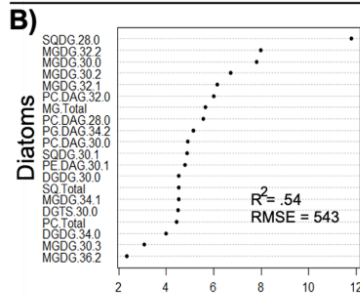
Recycling of PC and BL under N-limitation

Recycling of MG under high pH/low pCO₂, or anaerobiosis

Increased proportion of DG and SQ under thermal stress or high pH/low pCO₂

Increased proportion of SQ under shaded conditions

Recycling of MG and PG under high growth conditions



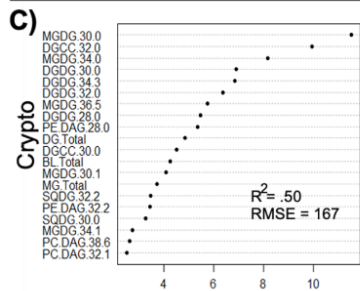
MG, SQ, PC

Recycling of BL under N-limitation

Increased proportion of SQ under thermal stress, shaded conditions, and high pH/low pCO₂

Increased proportion of MG for photoprotective and antioxidant mechanisms

Recycling of PG under high growth conditions



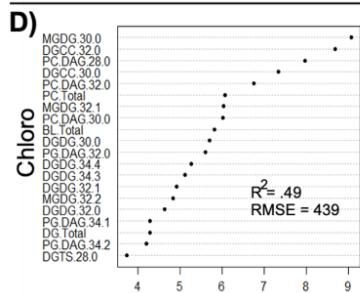
BL, DG, MG

Recycling of PC under N-limitation

Enhanced DG under thermal stress

Enhanced MG for photoprotective and antioxidant mechanisms

Recycling of SQ and PG under high growth conditions

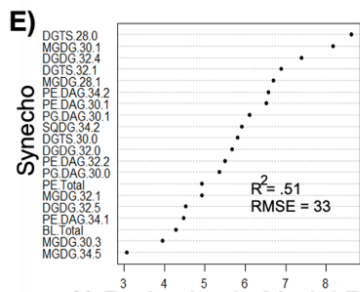


PC, BL, DG

Recycling of MG under high pH/low pCO₂ or anaerobiosis

Enhanced DG under thermal stress

Recycling of SQ, MG, and PG under high growth conditions



PE, BL

Recycling of PC under N-limitation

Recycling of MG under high pH/low pCO₂ or anaerobiosis

Increased proportion of SQ under shaded conditions

Recycling of SQ, MG, and PG under high growth conditions

% Reduction in Model RMSE

1484

1485 **Figure 8: Random Forest-based identification of the 15 most important individual IPLs in the prediction of phytoplankton groups.**
1486 **Dominant IPL classes and the potential remodeling advantages for each group are summarized. The nomenclature of IPL molecules**
1487 **follows that of the main text, starting with the type of headgroup, followed by the number of carbon atoms in fatty acid chains, and**
1488 **the total number of double bonds in the fatty acid chains. The root mean square error (RMSE) of random forest models is defined**
1489 **as ng/L of chl-a, and coefficient of determination (R^2) provided for each model fit.**